Exploratory genotype–phenotype correlations of facial form and asymmetry in unaffected relatives of children with non-syndromic cleft lip and/or palate

Steven F. Miller[1,*], **Seth M. Weinberg**[2], **Nichole L. Nidey**[3], **David K. Defay**[4], **Mary L. Marazita**[2], **George L. Wehby**[5], and **Lina M. Moreno Uribe**[1,6,*]

[1]Dows Institute for Dental Research, College of Dentistry, University of Iowa, Iowa City, IA, USA

[2]Center for Craniofacial and Dental Genetics, Department of Oral Biology, University of Pittsburgh, Pittsburgh, PA, USA

[3]Department of Pediatrics, University of Iowa, Iowa City, IA, USA

[4]Orthodontics Private Practice, Kaysville, UT, USA

[5]Department of Health Management and Policy, School of Public Health, University of Iowa, Iowa City, IA, USA

[6]Department of Orthodontics, College of Dentistry, University of Iowa, Iowa City, IA, USA

Abstract

Family relatives of children with nonsyndromic cleft lip with or without cleft palate (NSCL/P) who presumably carry a genetic risk yet do not manifest overt oral clefts, often present with distinct facial morphology of unknown genetic etiology. This study investigates distinct facial morphology among unaffected relatives and examines whether candidate genes previously associated with overt NSCL/P and left–right body patterning are correlated with such facial morphology. Cases were unaffected relatives of individuals with NSCL/P ($n = 188$) and controls ($n = 194$) were individuals without family history of NSCL/P. Cases and controls were genotyped for 20 SNPs across 13 candidate genes for NSCL/P (*PAX7, ABCA4-ARHGAP29, IRF6, MSX1, PITX2*, 8q24, *FOXE1, TGFB3* and *MAFB*) and left–right body patterning (*LEFTY1, LEFTY2, ISL1 and SNAI1*). Facial shape and asymmetry phenotypes were obtained via principal component analyses and Procrustes analysis of variance from 32 coordinate landmarks, digitized on 3D facial images. Case–control comparisons of phenotypes obtained were performed via multivariate regression adjusting for age and gender. Phenotypes that differed significantly ($P < 0.05$) between cases and controls were regressed on the SNPs one at a time. Cases had significantly ($P < 0.05$) more profile concavity with upper face retrusion, upturned noses with obtuse nasolabial angles, more protrusive chins, increased lower facial heights, thinner and more retrusive lips and more

Correspondence Lina M. Moreno Uribe, Dows Institute for Dental Research, N401 Dental Science Building, University of Iowa, Iowa City, IA 52242, USA. T: +1 319 3358912; lina-moreno@uiowa.edu.
*These authors contributed equally to this manuscript.

protrusive foreheads. Furthermore, cases showed significantly more directional asymmetry compared to controls. Several of these phenotypes were significantly associated with genetic variants ($P < 0.05$). Facial height and width were associated with *SNAI1*. Midface antero-posterior (AP) projection was associated with *LEFTY1*. The AP position of the chin was related to *SNAI1, IRF6, MSX1 and MAFB*. The AP position of the forehead and the width of the mouth were associated with *ABCA4–ARHGAP29* and *MAFB*. Lastly, facial asymmetry was related to *LEFTY1, LEFTY2 and SNAI1*. This study demonstrates that, genes underlying lip and palate formation and left–right patterning also contribute to facial features characteristic of the NSCL/P spectrum.

Keywords

facial asymmetry; genotype-phenotype correlations; morphometrics; NSCL/P; 3D morphology

Introduction

Non-syndromic cleft lip with or without cleft palate (NSCL/P) is a common craniofacial birth defect present in about 1 in 700 live births (Mossey et al., 2009). The incidence of NSCL/P varies by ancestry with rates of 1 in 500 live births in Asian and Native American populations, and rates of 1 in 2400 in African-based populations (Kirschner & LaRossa, 2000; Arosarena, 2007). Clinically, NSCL/P imposes a significant burden in affected individuals on many aspects of everyday life such as eating, speech and facial appearance, and thus significantly increases overall health care needs (Wehby & Cassell, 2010). Although significant progress has been made in understanding the genetic etiology of syndromic orofacial clefting (see review, Marazita, 2012) the identification of genetic variants etiological for NSCL/P has progressed at a slower pace due to its multifactorial nature (Dixon et al., 2011).

A key to understanding the etiology of NSCL/P lies in discerning the complex spectrum of subphenotypic expression of this condition, not only in individuals presenting overt clefts, but also in their seemingly unaffected close relatives with whom they share a portion of their genome and who could also be affected with less apparent features of the subphenotypic spectrum of NSCL/P. Studies have begun to unravel the complex phenotypic expression of NSCL/P beyond overt clefts, with promising results and possibilities for future research (Weinberg et al., 2008a, b; Weinberg et al., 2009). Subphenotypes of clefting studied previously can be categorized as either postcranial or craniofacial. Examples of postcranial subphenotypes include a preponderance of non-right-handedness, a higher incidence of slower forming or rare fingerprints and increased fluctuating asymmetry (FA) in dermatoglyphic patterns (Weinberg et al., 2006). Craniofacial subphenotypes include distinct craniofacial dimensions and facial morphology patterns, orbicularis oris muscle (OOM) discontinuities, dental anomalies, velopharyngeal incompetency, lip whorls, brain structure and vertebral anomalies, and both fluctuating and directional asymmetry (DA) that could be manifested in facial and dental traits (Weinberg et al., 2006; Neiswanger et al., 2009).

This study focuses on distinct facial morphology patterns in addition to aspects of facial asymmetry present in the relatives of children with NSCL/P. The majority of NSCL/P studies involving craniofacial dimensions and facial morphology patterns in unaffected relatives of children with clefts have relied mostly on lateral and PA cephalograms (McIntyre & Mossey, 2002, 2010; Weinberg et al., 2006). Despite a few inconsistent results, studies have shown that seemingly unaffected relatives of individuals with NSCL/P present with narrower cranial vaults, longer cranial bases, wider, shorter and more retrusive upper faces, longer and more protrusive lower faces, wider soft tissue noses and wider nasal cavities than controls (McIntyre & Mossey, 2002; Maulina et al., 2006; Weinberg et al., 2006) regardless of ethnic ancestry (Otero et al., 2012). Some of these features largely resemble those seen in unrepaired patients with overt clefts of the lip and palate. In particular, cephalometric studies of unrepaired patients have shown that affected individuals present with decreased vertical and antero-posterior dimensions in the maxilla, downward and backward rotation of the mandible with a very steep mandibular plane, reduced posterior facial height, and increased anterior facial height giving the appearance of bimaxillary retrusive faces (Bishara et al., 1986; da Silva Filho et al., 1998; Liao & Mars, 2005), supporting the presence of distinct facial morphology in cleft risk carriers both with and without overt clefts.

More recently, work has been undertaken to examine these morphological differences using three-dimensional imaging and shape analysis methods including geomorphometric methods (GM) (Weinberg et al., 2008a, b, 2009). These studies have shown that unaffected male relatives present with greater upper facial and cranial base widths, increased lower facial height, and decreased upper facial height compared to controls. Female relatives also have shown similar facial patterns, with increased upper facial width, more lateral placement of the alar cartilage, and midfacial retrusion (Weinberg et al., 2008a, b, 2009).

In addition to the morphometric studies described above, work has also been done to examine overall levels of body (Werner & Harris, 1989; Neiswanger et al., 2002, 2005) and craniofacial bilateral asymmetry (McIntyre & Mossey, 2010) in NSCL/P families. The effects of asymmetry on the phenotype can be classified as either FA or DA (Klingenberg et al., 2002; Weinberg et al., 2006). FA is defined as random deviations from symmetry within a form such as the human face that has object symmetry (i.e. symmetry along a central axis; Valen, 1962; Klingenberg et al., 2002; Weinberg et al., 2006). In contrast, DA involves structures that are systematically larger or preferentially asymmetric on one side of the body vs. the other (Valen, 1962). FA results as a compromise between the processes of developmental noise (a set of processes that cause perturbations in normal development) and developmental stability (processes that prevent or nullify disruption in the developmental process). This is illustrated by a tendency for FA to increase if there is: (i) an increase in developmental noise or (ii) a decrease in developmental stability within an organism (Palmer & Strobeck, 1992; Palmer, 1994). Since FA in the craniofacial phenotype can be indicative of developmental perturbations and instability, it is an important component in examining the cleft phenotype. Studies have found increased levels of FA in dermatoglyphs and dental traits in individuals with clefts and their unaffected relatives compared with control populations (Weinberg et al., 2006). In addition, dental anomalies including bilateral asymmetrical expression of missing teeth have been found more often in individuals with

clefts than in controls (Sofaer, 1979; Nystrom & Ranta, 1988; Werner & Harris, 1989; Weinberg et al., 2006; Menezes & Vieira, 2008), suggesting examples of FA as part of the phenotypic spectrum of NSCL/P.

Overt clefts of the lip can be unilateral or bilateral, with unilateral clefts being twice as common as bilateral clefts (Kirschner & LaRossa, 2000; Arosarena, 2007). In unilateral cleft cases, there is a strong predominance of left side unilateral clefts over the right side (Mossey et al., 2009). Given the left side predilection, it can be hypothesized that asymmetry and, specifically, left-side DA may be a subphenotype of the NSCL/P spectrum in affected individuals as well as their seemingly unaffected relatives (Neiswanger et al., 2002, 2005; Weinberg et al., 2006). A few DA studies have found DA in parents of children with NSCL/P (McIntyre & Mossey, 2002, 2010) and, interestingly, some have found positive correlations between the side of DA within the nasomaxillary complex of the parents and the side of the cleft in their affected children (Yoon et al., 2003).

Studies of NSCL/P susceptibility genes have mostly utilized a qualitative rather than a quantitative definition to designate affection status for patients with overt clefts. These studies have shown consistent results for the presence of etiological variants nearby or within genes and loci *MSX1, TGFB3* (Lidral et al., 1998), *IRF6* (Zucchero et al., 2004; Vieira et al., 2007; Wu et al., 2010), *FGF* and *FGFR* families (Bei & Maas, 1998; Riley & Murray, 2007; Riley et al., 2007; Vieira et al., 2007), *BMP4* (Bei & Maas, 1998; Suzuki et al., 2009), *FOXE1* (Moreno et al., 2009; Venza et al., 2011), *ADH1C* (Chevrier et al., 2005), *MAFB* and *ABCA4-ARGHAP 29* (Beaty et al., 2010), *PAX7* (Mansouri et al., 1996; Dahl et al., 1997), and 8q24 (Birnbaum et al., 2009; Beaty et al., 2010; Mangold et al., 2010; Boehringer et al., 2011). In addition, recent studies have found that some of these genes, including *BMP4, MSX1, TGFB3 and* 8q24, can also modulate the expression of the phenotypic spectrum in patients with NSCL/P including dental anomalies (van den Boogaard et al., 2000; Slayton et al., 2003; Modesto et al., 2006; Suzuki et al., 2009), microform cleft lip, and other aspects of cleft craniofacial facial variation such as the bizygomatic distance (Boehringer et al., 2011). Moreover, animal knockout models for some of these genes present with craniofacial dysmorphology in addition to the presence of overt oral clefts (Table 1).

Candidate genes implicated in left–right body patterning such as *PITX2* (Lin et al., 1999; Boorman & Shimeld, 2002), *ISL1* (Yuan & Schoenwolf, 2000), *SNAI*1 (Paznekas et al., 1999), *LEFTY1 and LEFTY2* (Meno et al., 1997) are also of interest given the findings that FA and DA are part of the cleft phenotype. In addition, *PITX2, ISL1 and SNAI1* have very specific roles during the formation of the lip, palate and anterior teeth as well as for facial expression and masticatory muscles (Table 2) and therefore these genes may be responsible for patterns of DA and FA in addition to other distinct facial features within the large phenotypic variation present in individuals with NSCL/P risk.

There is an extensive amount of literature on the phenotypic spectrum of NSCL/P (McIntyre & Mossey, 2002; Maulina et al., 2006; Weinberg et al., 2006) and the role of key cleft and craniofacial candidate genes in NSCL/P overt clefts (Dixon et al., 2011). However, there is a lack of studies focusing on how particular genotypes of these genes and loci and genes

involved in left–right body patterning influence the phenotypic expression of the clefting spectrum in individuals with clefts and their close relatives. Only a handful of recently published studies not focused on NSCL/P have attempted to study genetic associations with facial morphology in general samples, via GWAS and 3D facial imaging methods (Boehringer et al., 2011; Liu et al., 2012). More studies are needed to understand phenotype–genotype correlations not only in the general population but also in individuals carrying genetic risk for craniofacial conditions, especially NSCL/P. The purpose of this study is to identify features of distinct facial morphology and bilateral facial asymmetry present in seemingly unaffected relatives of children with NSCL/P and to explore the role of cleft and left–right body patterning candidate genes in these distinct features. This effort will help prioritize genetic pathways important in the overall cleft phenotypic spectrum beyond overt clefts for future research.

Materials and methods

The study protocol was reviewed and approved by the Institutional Review Board at the University of Iowa. The study sample consisted of 188 unaffected relatives ('cases'; $n = 119$ parents and $n = 69$ siblings) of children with NSCL/P and 194 control individuals with no family history of oral clefts or facial surgeries (Table 3). Study individuals were recruited in Iowa as part of the Iowa Oral Cleft Study. The majority of the sample ($n = 362$) self-reported their race as Caucasian; a minority ($n = 20$) reported their race as non-Caucasian, including Asian, African American, Native American or Alaskan Native, or other.

To maximize our statistical power and to capture common morphological features that are shared by unaffected relatives regardless of their sex or age, our main analysis combined all cases (and controls) adjusting for age and gender and accounting for family clustering as described below in detail. We also explored heterogeneity by age/gender stratifying the total sample into four subgroups by age category and gender. Our statistical analyses for case–control phenotype differences and genetic associations are described below in detail.

Facial morphology and asymmetry phenotypes

Facial phenotypes were generated from three-dimensional stereophotogrammetric images taken with a 3dMD imaging system (Lubbers et al., 2010). Stereophotogrammetry is an established tool for capturing facial surface phenotypic information that has been employed in several other similar studies (Seager et al., 2009; Weinberg et al., 2009; Incrapera et al., 2010). A total of 32 standard facial 3D coordinate landmarks were collected from the 3dMD facial images (Fig. 1, Table 4) and were verified for reliability in a subsample of 15 individuals digitized twice with 2 weeks between digitizing sessions. *T*-tests, Euclidean distance (ED) and intra-class correlation methods (ICC; Landis & Koch, 1977) were employed to evaluate landmarking error between the two digitizing attempts. The average ED obtained was 1 mm; however, landmarks Glabella, Pogonion and Gnathion showed EDs of above 2 mm. *T*-tests were used to evaluate whether the distances between coordinate locations from both attempts were significantly different from zero. A total of 32 *t*-tests per coordinate (X, Y and Z) were calculated. We considered the *t*-test significant at $P = 0.001$ $(0.05/32 = 0.001)$. None of the coordinates were significantly different from zero at $P =$

0.001. Overall results from ICC showed values above 0.8, indicating good to excellent reliability except for the landmark Pogonion (ICC = 0.77). Efforts were made to resolve the discrepancies for Glabella, Pogonion and Gnathion until good reliability was obtained.

Once all facial images were digitized, coordinates of the land-mark configurations were subjected to GM analyses for the pooled and stratified samples separately using MORPHOJ (Klingenberg, 2011). Facial landmark configurations in this study have object symmetry, meaning that both the left and right side of the face (divided by the midsagittal plane) are mirror images of each other. Following the methodology in MORPHOJ for data with object symmetry (Mardia et al., 2000; Klingenberg et al., 2002) all original landmark configurations were reflected and relabeled. Subsequently, both the original and their relabeled mirrored configurations were registered using the Procrustes fit procedure in MORPHOJ and the total shape variation was partitioned into components of symmetric and asymmetric shape variation. Symmetric components of shape indicate variation among individuals in the average between their original and reflected landmark configurations. Despite any left–right asymmetry present in the original landmark configuration in any given individual, the average configuration between the original and its reflection is always a symmetric shape (Klingenberg et al., 2002). In symmetric variation, bilateral paired facial landmarks can vary in any direction but midfacial unpaired landmarks can only vary along the midsagittal plane. On the other hand, the asymmetric component of shape variation quantifies the differences between the original and reflected configuration within individuals. For the paired landmarks, asymmetry can be in any direction, but for the unpaired landmarks variation can only be in a direction perpendicular to the midsagittal plane (Klingenberg et al., 2002). Covariance matrices for both the symmetric and asymmetric components were generated and subsequently submitted separately to principal component analyses (PCA) to determine components of symmetric and asymmetric facial shape variation (Mardia et al., 2000; Klingenberg et al., 2002). Scree plots of the PCA were used to determine the number of symmetric and asymmetric shape components that explained the most variation for further analysis.

The resultant components were tested for differences between cases and controls in the pooled sample via multivariate linear regression by regressing the components, one at a time, on an indicator for case vs. control status, sex, and indicators for five age categories (C1: 0–10 years, C2: 11–19 years, C3: 20–29 years, C4: 30–39 years and C5: 40–70 years). To account for family clustering, the regression model included family–random effects that allowed for dependence between individuals in the same family (Wooldridge, 2002). The random-effect models were estimated in STATA (StataCorp, 2011). Next, we explored differences in the phenotype principal components between cases and controls stratifying the sample by age and sex into four groups: (i) adult females (> 18 years) including mothers of affected children and adult female controls; (ii) adult males (> 18 years) including fathers of affected children and adult male controls; (iii) subadult females (18 years), including sisters, of affected children and control female children; and (iv) subadult males (18 years), including brothers of affected children and control male children. Linear regression was used, controlling for age as a continuous variable (in years). Since only a few children were blood relatives within each stratified subgroup, it was not feasible to include random-effects to account for relatedness similar to the pooled analysis. Instead, we limited each

subgroup to non-related individuals by excluding the younger blood-related children. Therefore, none of the individuals within the stratified analysis was blood-related.

In addition to PCA, a Procrustes analysis of variance (ANOVA) assuming an isotropic model (equal variance around each landmark position) and a multivariate analysis of variance (MANOVA) approach in a non-isotropic model (non-equal variance) were performed to quantify the effects of 'Individuals' (symmetric component), 'Sides' or DA, and 'Individuals × Sides' or FA in the overall shape variation of the pooled sample and for each sample subgroup in the stratified analysis (Mardia et al., 2000; Klingenberg et al., 2002).

Directional asymmetry was calculated as the mean difference between each configuration and its reflection, which is equivalent to the average difference between sides. Overall DA was computed as the average asymmetry across all individuals in both the pooled and the stratified samples. DA comparisons between cases and controls were performed via discriminant function analyses and permutation tests in MORPHOJ utilizing Procrustes distances (a measure of the absolute magnitude of shape differences which does not take into account the direction of the mean differences) and also the T-square statistic, which does take into account the extent of variation in different directions of space (Klingenberg & Monteiro, 2005; Klingenberg et al., 2010).

Fluctuating asymmetry measures the dispersion of left–right differences within individuals; in other words, FA corresponds to the deviation of each individual's asymmetry from the overall average of asymmetry in the sample. In this study, individual FA scores were calculated in Procrustes distances and Mahalanobis distances (scaled relative to the variation of asymmetry in the sample) utilizing MORPHOJ. These individual FA scores were also compared between cases and controls both in the pooled and stratified samples using the same regression models described above for the principal component phenotypes.

Finally, we evaluated centroid size as a proxy to measure the overall size of a face. Centroid size was calculated as the square root of the sum of squared distances between the centroid and all other points in the landmark configuration. We compared centroid size between cases and controls using the same regression models described above for the principal components and FA scores.

In summary, the phenotypic data derived from the application of GM methods in both the pooled and the stratified samples included principal components of symmetric and asymmetric shape variation, overall levels of DA, individual FA scores and centroid size. As described above, case–control differences in phenotypes were performed via discriminant function analysis for DA phenotypes with MORPHOJ and multivariate regression analyses for all other individuallevel phenotypes, accounting for family dependence and adjusting for sex and age group in the pooled analysis and continuous age in the sex/age stratified analyses. Phenotypes that were found to vary significantly ($P < 0.05$) between cases and controls were subsequently examined for association with the genetic variants as described below.

Genetic analysis

Genotypes for 20 SNPs across 13 candidate genes and loci (Table 5) implicated in craniofacial variation and clefting (*PAX7, ABCA4-ARHGAP29, IRF6, MSX1*, 8q24, *FOXE1, TGFB3* and *MAFB*) as well as left/right body patterning (*LEFTY1*, *LEFTY2*, *ISL1*, *PITX2* and *SNAI1*) were generated via Taqman assays from Applied Biosystems (Foster City, CA, USA). Allele frequencies were calculated with the NCSS statistical package (Hintze, 2006) and SNP genotypes were recoded based on the number of rare alleles present (i.e. 0, 1 or 2 copies of the rare allele present) in an individual's genotype.

Multivariate regressions were employed to test for the association between each of the 20 SNPs and the phenotypes that varied significantly ($P < 0.05$) between cases and controls from the analyses described above. Similar to the regressions of the phenotypes on case–control status described above, the regressions of phenotypes on SNPs controlled for sex and age groups as covariates and included random effects to account for familial dependence.

Next, we evaluated whether differences in phenotypes by case–control status were explained by differences in allele frequencies between cases and controls. For each phenotype that was significantly associated with a SNP in the above-described regressions, we re-estimated the regression for that phenotype and the significant SNP, adding case/control status as a covariate (in addition to the gender and age covariates). We then compared the coefficient of the case/control status in this regression with that in the regression model excluding the SNP (i.e. the original regression model comparing the phenotype by case–control status) to evaluate whether the SNP explained any of the case–control difference in the phenotype.

Results

We first present the results for significant phenotypic differences and association with the genetic variants in the pooled sample. Next, we summarize the results for the analysis stratifying by age/gender.

Pooled sample

Phenotypic differences—Principal component analyses of the symmetric and asymmetric component of shape variation in the pooled sample resulted in seven symmetric and eight asymmetric components explaining 72.2% and 65% of the shape variation, respectively. These components, along with overall DA, individual-level FA scores and centroid size, were compared between cases and controls as described above. Of all these phenotypic measures, five varied significantly ($P < 0.05$) between cases and controls: three were principal components representing aspects of symmetric shape variation, one was a principal component capturing asymmetric shape variation, and the fifth was overall DA (Tables 6–8). We discuss each of these differences below.

Symmetric principal component 1 (SymmPC1) explained 19.6% of symmetric shape variation (Figs 2 and 3). With this component, cases tended to have a longer lower anterior facial height and a more protrusive chin, whereas controls had a greater tendency for a shorter, more convex face. Symmetric principal component 3 (SymmPC3) explained 12% of symmetric shape variation and revealed that cases had a tendency for a less protrusive nose

and overall mid-face face retrusion; controls showed the opposite morphology with midface face protrusion. Symmetric principal component 7 (SymmPC7) explained 3.6% of symmetric shape variation and showed cases to have a more protrusive forehead, a shorter nose and a steep mandibular plane. Asymmetric principal component 4 (AsymmPC4) captured 6.6% of the variation in the asymmetric component of shape and revealed a tendency for a left deviation of the base of the nose and chin among cases and the opposite morphology among controls (Fig. 4).

Procrustes ANOVA shape results indicated that DA and case–control status were the main sources of variation for the pooled sample. FA had the lowest effect on shape variation in the Procrustes ANOVA and subsequent regression analyses of individual FA scores showed no case–control differences. MANOVA results confirmed ANOVA findings, indicating that case–control status had a significant effect in the symmetric component and that both case–control status and DA had large effects in the asymmetric component of shape variation (Table 7). Discriminant function analysis of the asymmetric component of shape variation indicated greater DA among cases than controls (difference between means in Procrustes distance = 0.00276566, $P = 0.0338$; and Mahalanobis distance = 0.8696, $P = 0.0114$, after 10 000 permutations; Table 8). Given the difference in DA levels between cases and control, we evaluated whether DA differences varied by the laterality of the cleft present in the 1st degree relatives of cases by recoding cases into two groups: (i) relatives of an individual with a unilateral cleft lip and (ii) relatives of an individual with bilateral cleft lip. These two case groups were compared with the total control sample and with each other. Interestingly, levels of DA were significantly different between relatives of individuals with unilateral clefts compared with controls and almost significantly different when comparing relatives of unilateral vs. bilateral clefts. However, there was no difference in DA levels between relatives of individuals with bilateral clefts and controls (Table 8).

Phenotype–genotype correlations—Significant genotype–phenotype associations ($P < 0.05$) from the regressions described above (for phenotypes that varied significantly between cases and controls) were identified for SNPs in genes *SNAI1, LEFTY1, IRF6, MAFB* and *MSX1* (Table 6). *SNAI1* was associated with SymmPC1; the rare allele for the *SNAI1* SNP rs6012791 was associated with 'control-like' morphology with shorter and more convex faces. When case–control status was added as a covariate to the regression of SymmPC1 on *SNAI1* SNP rs6012791 (and the age and sex covariates), the β coefficient of case–control status was 7.1% lower than that in the model excluding the SNP, indicating that differences in allele frequencies for this *SNAI1* SNP partially explain (~7%) the phenotypic difference captured by SymmPC1 between cases and controls.

LEFTY1 SNP rs3766941 was associated with SymmPC3, which captured variation in maxillary protrusion or retrusion; the rare allele of the SNP was associated with 'control-like' morphology with upper face protrusion. When adding case–control status to this regression and comparing its coefficient with that of the model excluding the SNP, the coefficient slightly increased, indicating that even though *LEFTY1* was associated with SymmPC3 in the pooled sample, it did not explain any of the difference in this phenotype between cases and controls.

SNPs in *IRF6* rs2235371, *MSX1* rs12532 and *MAFB* rs11696257 were associated with SymmPC7. The rare alleles of *IRF6* rs2235371 and *MSX1* rs12532 were related to 'control-like' morphology including retrusive foreheads, flat mandibular planes and convex profiles. The *IRF6* and *MSX1* SNPs explained about 6.6 and 0.8% of the difference in SymmPC7 between cases and controls, respectively. Lastly, the rare allele of *MAFB* rs11696257 was associated with 'case-like' morphology on SymmPC7 (Figs 2 and 3), but this SNP did not explain any of the difference in this phenotype between cases and controls. Finally, DA was significantly ($P < 0.05$) associated with SNPs in *ABCA4-ARHGAP29, LEFTY1, LEFTY2, MSX1* and *SNAI1*. Unlike the regression models for phenotypes measured at the individual-level, the MORPHOJ software for analyzing DA, a group-level trait, does not allow for evaluating the extent to which these SNPs explain case–control differences in DA levels.

Stratified analyses

Case–control comparisons of phenotypic data and phenotype– genotype correlations were performed in four separate subsamples as described above (Table 9): (i) adult males: case fathers and control adult males (18 years and older), (ii) adult females: case mothers and control adult females (18 years and older), (iii) subadult males: case male siblings and control subadult males (younger than 18 years) and (iv) subadult females: case female sisters and control subadult females (younger than 18 years). We summarize the main results for each of these subsamples below.

Adult male sample—PCA analyses resulted in eight symmetric and nine asymmetric components explaining 75.1 and 74.5% of the total variance in this subgroup, respectively. None of these components showed significant differences ($P < 0.05$) by case–control status. Procrustes ANOVA and MANOVA results also revealed no differences in DA and FA between cases and controls in this subgroup (Table 10).

Adult female sample—PCA analyses resulted in 10 symmetric and 11 asymmetric components that accounted for 82.5 and 75% of the symmetric and asymmetric total variance in this subgroup. SymmPC6, SymmPC10 and AsymmPC5 were significantly different (at $P < 0.05$) between cases and controls (Table 9). SymmPC6 explained 4.7% variance and captured variation in facial height, mouth width, nasal projection and concavity vs. convexity of the facial profile. Adult female cases showed increased lower facial height and decreased midfacial height, wider mouths, more superior placed and projecting noses, slightly narrower faces and a concave profile compared with controls. SymmPC10 accounted for 2.5% of the total variance. On this component, cases tended to exhibit wider commissures, longer philtrums, upturned noses and slightly more prominent chins. Conversely, controls had significantly narrower commissures, shorter philtrums and down-turned noses inclined anteriorly near the point of nasion (Figs 5 and 6).

AsymmPC5 explained 6% of the variation and showed that case mothers had a tendency for left-oriented chins and superior portion of the nose, with a slightly right orientation of the philtrum (Fig. 7).

Procrustes ANOVA and MANOVA showed that DA and case–control status made the largest contribution to overall shape variation in the adult female sample followed by symmetric

variation and lastly FA (Table 10). However, there was no significant difference in overall DA between cases and controls. In contrast, centroid size and Mahalanobis FA scores varied significantly by case–control status (Table 9). Adult female cases had larger centroid sizes overall ($P = 0.002$) and greater FA when compared with controls ($P = 0.04$).

Significant ($P < 0.05$) phenotype–genotype associations were found for *ABCA4-ARHGAP29* and *LEFTY1* (Table 9). SymmPC10 was associated with *ABCA4-ARHGAP29* rs560426 ($P = 0.0005$) with the rare allele related to a 'case-like' morphology with wider mouths, and less projecting and upturned noses (Figs 5 and 6). *LEFTY1* rs360059 was associated with AsymmPC5 ($P = 0.042$; Table 9), with the rare allele related to a 'case-like' morphology with left-oriented base of the nose and chin. Additional regression models were explored for SymmPC10 and AsymmPC5, including case/control status and SNPs rs560426 (*ABCA4-ARHGAP29*) and rs360059 (*LEFTY1*), respectively. Comparison between b coefficients for models excluding and including the SNPs indicated that the variation on both phenotypes cannot be explained by the difference in allele frequencies by cases and controls.

Subadult male sample—PCA analyses resulted in seven symmetric and 10 asymmetric principal components, each set explaining about 74% of the total shape variation in this subgroup. Of these, only SymmPC5, which accounted for 5.8% of the variation, was significantly related to case–control status ($P = 0.04$; Table 9). On this component, cases showed less projecting noses, marked midfacial retrusion, increased facial height and narrower faces and mouths compared with controls (Fig. 8).

Procrustes ANOVA and MANOVA showed that overall DA and symmetric shape variation had the largest influence on overall shape variation within this subgroup (Table 10B). However, there were no significant differences in overall DA and FA between cases and controls. Also, none of the SNPs were significantly related to SymmPC5 – the only phenotype that varied by case–control status in this subgroup.

Subadult female sample—PCA resulted in nine symmetric and nine asymmetric components explaining 79.5 and 75% of the total shape variation in this subgroup, respectively. Of these, only SymmPC2 and SymmPC9 showed significant differences ($P = 0.049$ and $P = 0.033$, respectively) between cases and controls. SymmPC2 explained 16.3% of the total variance and accounted for differences in facial and mouth width, chin and nasal projection. On this component, cases showed reduced nasal projection, smaller and retruded chins, and narrower mouths. SymmPC9 explained 3.8% of the total variation and captured overall facial width and height and, to a lesser degree, midfacial and chin projection. It revealed cases to have longer faces, steeper mandibular planes and more concave profiles compared with wider and shorter faces among controls (Figs 9 and 10).

Procrustes ANOVA and MANOVA showed that DA and case–control status made the largest contribution to overall shape variation in the subadult female sample followed by symmetric variation and lastly FA (Table 10). However, DA and FA did not vary significantly between cases and controls in this subgroup, nor did centroid size.

A SNP on *LEFTY1* (rs360059) was associated ($P = 0.037$) with SymmPC2; the rare allele was related to 'control-like' morphology with more prominent and projecting noses and chins and narrower faces. But this SNP did not explain any of the difference in SymmPC2 by case–control status. None of the SNPs were related to SymmPC9 in this subgroup.

Discussion

Facial morphology differences between cases and controls

Previous studies have shown that seemingly unaffected relatives of NSCL/P individuals have shorter and more retrusive upper faces, longer and more protrusive lower faces, wider soft tissue noses and wider nasal cavities compared with controls (McIntyre & Mossey, 2002; Maulina et al., 2006; Weinberg et al., 2006, 2008a, b, 2009). In the current study we found several phenotypic differences between cases and controls that mirrored previous studies. In general, findings for symmetric shape variation in our pooled case sample showed profile concavity with upper face retrusion, an upturned nose with an obtuse nasolabial angle, a protrusive chin, increased lower facial height, thinner and more retrusive lips, and slightly more protrusive foreheads compared with controls. Our findings in subgroups stratified by age/gender are overall similar with some features that are specific to the subgroup. For example, our male cases showed more retrusive midfaces, decreased upper face height and increased lower face height compared with controls, regardless of the age group evaluated, yet these features were only statistically significant (at $P < 0.05$) for the subadult males (Fig. 8). For females, some similarities are noted between our findings and previously published work, such as increased lower face heights, projecting chins and steep mandibular planes. In addition, we found new and previously unreported differences for adult female cases including larger faces (i.e. larger centroid sizes), a tendency for an obtuse nasolabial angle, and bimaxillary retrusion resulting in a 'dished in' appearance with retrusion in the midface and in the superior aspect of the nose and forehead (Fig. 5). The subadult female group also showed the obtuse nasolabial angle and the bimaxillary retrusion, yet faces were slightly wider than the controls (Figs 9 and 10).

Overall, facial features observed in our case relatives are very similar to those observed in cephalometric studies of unrepaired patients (Bishara et al., 1986; da Silva Filho et al., 1998; Liao & Mars, 2005). In a study by da Silva Filho et al. (1998). Males and females with bilateral clefts were found to have more bimaxillary retrusion and increased nasoloabial angle than controls, features that resemble those we found in case relatives. Thus, our results combined with those of the previous studies indicate a pattern of craniofacial features characterized mostly by a shorter and a more retrusive upper face, a longer lower face, and a downward and backward rotation of the mandible which seems not to be a consequence of surgical procedures, as these are observed in unaffected relatives, but rather a feature of the phenotypic spectrum of NSCL/P in individuals with cleft genetic risk.

In terms of asymmetric variation, both DA and FA have been found in the craniofacial complex of normal individuals (Johnson et al., 2008) and in individuals with craniofacial anomalies such as fetal alcohol syndrome (Klingenberg et al., 2010) and NSCL/P (Bock & Bowman, 2006). Moreover, one study of hard tissue asymmetry in parents of children with NSCL/P from PA cephs showed size and shape DA in the craniofacial complex (McIntyre &

Mossey, 2010). However, that study did not have controls without a family history of clefting to compare with affected relatives, making it unclear whether DA was more common in carriers of cleft risk (McIntyre & Mossey, 2010). More recently, FA was also identified in relatives of children with clefts from different ancestral backgrounds (Otero et al., 2012). In the current study, we identified DA to be the main source of asymmetric shape variation in our sample, followed by FA. The pooled analysis showed significantly different levels of DA in cases compared to controls in Procrustes distances (PD) ($P = 0.037$) and T-square (TS) statistics ($P = 0.011$). When examining DA differences by the cleft laterality of the affected child, we found that levels of DA differed significantly between relatives of children with unilateral clefts and controls ($P = 0.046/0.006$ for PD and TS, respectively) and almost significantly when compared to relatives of bilateral cases ($P = 0.671/0.067$ for PD and TS, respectively). However DA was not significantly different between relatives of bilateral cases and controls (Table 8). This finding for DA requires replication in other samples; however, it is intuitive and consistent with the theory that DA is more relevant for those who carry risk for unilateral clefts than for bilateral clefts.

In contrast, differences in FA were less prominent in our sample. Only one asymmetric component of variation in the pooled sample (AsymmPC4), capturing FA in the nose, philtrum of the lip and the chin, was significantly different between cases and controls (Fig. 4). This difference was also found among adult females captured by AsymmPC5 (Fig. 7). Only adult female cases had significantly higher FA scores than controls (FA score differences were insignificant in the pooled sample), suggesting potential heterogeneity in FA differences between cases and controls by age/gender.

Even though our study is exploratory in many aspects and its sample size is comparable to, and in certain cases larger than, previous studies in this area, our sample is still relatively small and limited in power to detect all differences at a conservative type-1 error level. We followed a type-1 error of 5% to summarize our findings, but recognize that it is important to consider an adjustment for multiple testing before making robust statistical conclusions. One approach commonly followed in similar studies would be to use a Bonferroni-type correction based on the number of phenotypes tested: this would reduce the significance level to 0.003, given that we test up to 14 phenotypes between cases and controls ($P = 0.05/14$ maximum number of phenotypes tested). Following this adjustment, only two findings of the several phenotypic differences significant at $P < 0.05$ between cases and controls have P-values below this adjusted significance threshold: AsymmPC4 in the pooled sample and centroid size in the adult female subgroup ($P < 0.003$; Tables 6 and 9). Therefore, even though our study points to several potential phenotypic differences, clearly larger samples are needed for a more definitive assessment.

Genetic associations with symmetric shape variation

Our analyses suggested that several aspects of symmetric shape variation, including protrusion/retrusion of the mid-face and chin, facial height and width, nose projection, and protrusion of the nasal base, which varied significantly between cases and controls were associated with SNPs in craniofacial and left–right body patterning genes. Some of these associations are worth highlighting and discussing. *SNAI1* was associated with facial height

and width and the anterior-posterior (AP) position of the chin. *SNAI1* is expressed throughout the palatal shelf mesenchyme with high levels of expression in the medial edge epithelium which is crucial in the fusion of palatal shelves. In addition, neural crest-specific *Snai1* deletion in *Snai2*$^{-/-}$ mice results in multiple craniofacial defects including cleft palate caused by failure of the mandible to move forward, similar to cases with Pierre Robin sequence, indicating that *SNAI1* is an important candidate for studying variation in facial morphology related to the NSCL/P spectrum. Interestingly, the *SNAI1* SNP explained up to 7% of the phenotypic difference between cases and controls on SymmPC1, a rather considerable effect given the multifactorial and complex etiology of facial phenotypes.

The AP position of the midface and facial asymmetry were associated with *LEFTY1*. The most studied role for *LEFTY1* is its function in L–R body patterning. Therefore the associations with facial asymmetry we found, including those with both DA and FA, were encouraging findings. However, the association with midfacial AP projections is less clear given current knowledge about *LEFTY1*. Future research is needed to confirm and, if so, explain the role of this gene in the antero-posterior growth of the midface.

The AP position of the chin was also associated with SNPs in *IRF6, MSX1* and *MAFB*. These associations of *IRF6* and *MSX1* with AP facial shape variation that we observed are consistent with the phenotypic expression of the null mice which present with shorter and rounded snouts and jaws in the case of *Irf6* nulls (Ingraham et al., 2006) and reduced overall length of the mandible in the *Msx1* nulls (Satokata & Maas, 1994). Our results with *MAFB* are also in line with the expression pattern of this gene in the craniofacial ecto-derm and neurocrest-derived mesoderm in mice during palatal shelf fusion; therefore, *MAFB* constitutes a good candidate for future studies of NSCL/P-specific craniofacial morphology (Beaty et al., 2010).

Interestingly, we found no associations between *PAX7* and symmetric shape phenotypes despite evidence that this gene is involved in maxillary and nasal development and has been implicated in cleft palate formation (Mansouri et al., 1996).

As for the case of analyzing phenotypic differences between cases and controls, our analyses of genetic associations with these differences are also considered exploratory and are limited by the study sample size to only capturing large associations. Therefore, even though we find several suggestive associations that are significant at $P < 0.05$, most of these would not be considered strictly significant when accounting for the multiple genetic tests. Indeed, if we apply a Bonferroni-type correction to the significance threshold for the 20 SNPs we tested, only two genotype–phenotype associations remain significant at $P = 0.0025$ ($P = 0.05/20$ SNPs): *IRF6* with SymmPC7 ($P < 0.001$) in the pooled sample and *ABCA4-ARHGAP29* with SymmPC10 in the adult female subgroup ($P = 0.0005$). Even though such associations involve phenotypes that explain a small percentage of the total facial variation, these findings in a rather limited sample size suggest that these two genes could be prioritized in future analyses of facial morphology in individuals with cleft risk. In addition, as a whole, our multiple findings of possible genetic associations with facial phenotypes highlight the value of pursuing the same research question and approach in larger and more powerful samples.

Genetic associations with asymmetric shape variation

Directional asymmetry and FA are key features in studying craniofacial anomalies, yet the biological mechanisms underlying these sources of asymmetry are still unclear and controversial. Although FA had been considered to be largely of environmental origin and DA to have a genetic basis, recent studies have shown evidence of genetic mechanisms for both (Leamy et al., 2000). Heritability studies of FA on a single trait have shown low heritability estimates (H = 0.03). However, when FA is measured by a composite of traits, FA heritability estimates increase to moderate levels (H = 0.3; Johnson et al., 2008). FA has also been considered a good measure of developmental instability, which is defined as the failure to produce optimal and precise outcomes in the generation of traits in different environments. Therefore, it is possible that variation in genes that play a role in the formation of the lip and palate can partly account for subtle left–right phenotypic differences in individuals carrying cleft risk either directly or by increasing susceptibility to environmental risk factors that interfere with the development of the craniofacial structures through a gene × environment interaction mechanism. Exploring such interactions with large samples and rich environmental data is an important avenue for future research.

Given the higher genetic heritability estimates for DA (as high as 0.21 for the sum of DA values for multiple characters combined; Leamy, 1999) and the specific genetic pathways that control the formation of asymmetric structures, it is reasonable to assume a genetic influence on DA (Palmer, 1994; Leamy et al., 2000) and to rule out DA as a good measure of developmental instability (Palmer, 1994). However, genetic studies for QTLs in mouse mandibles both utilizing multi-landmark measurements as well as GM methods have only shown a handful of QTLs with minor effects on DA and even less on FA of size and shape (Leamy et al., 2000; Klingenberg et al., 2001), suggesting small genetic contributions to both sources of asymmetry when single locus models (additive, dominant effects) are utilized. Theoretical models of FA have proposed genetic epistasis as the likely mechanism for FA in a bilateral trait for which different genes contribute to its overall development and formation (Klingenberg & Nijhout, 1999). This epistatic model was tested by Leamy et al. (2002) in a genome-wide scan for QTLs affecting FA in the centroid size of the mouse mandible. Strong evidence of genetic epistasis was observed, indicating that single locus models were underpowered to detect the genetic loci for FA in the mandible (Leamy et al., 2002). Similar models of genetic epistasis were later utilized to investigate FA of tooth size and shape. Once again, genetic epistasis was largely detected and, interestingly, most of the QTLs detected in the epistatic models were coincident with those controlling tooth size and shape (Leamy et al., 2005), rendering support to the theoretical model of Klingenberg & Nijhout (1999) that the same genes responsible for the formation of a bilateral trait may be responsible for the expression of FA in that trait.

Our findings of different levels of DA in relatives of individuals with unilateral clefts compared with controls or relatives of individuals with bilateral clefts are particularly interesting because they highlight a potential mechanism for DA in unilateral clefts. In the same vein, the associations of left–right body patterning genes, *LEFTY1, LEFTY2* and *SNAI1*, with DA could shed some light on potential pathways to be considered in future studies of facial asymmetry. The difference in FA scores between cases and controls and

association with *LEFTY1* were specific to adult females, suggesting potential heterogeneity by age/gender. However, these results need to be confirmed with larger samples.

Conclusion

In conclusion, our results demonstrate once again the presence of distinct craniofacial characteristics of facial shape and asymmetry in seemingly unaffected relatives of individuals with NSCL/P. Measuring these phenotypic differences may be useful for predicting risk. For example, regressing case–control status on the four individual-level phenotypes (three principal components for symmetric and one for asymmetric variation) that were significantly different between cases and controls shows that these phenotypes collectively explain ~8% of the risk of being a first degree relative of an individual with an oral cleft (adjusting for sex and age). This is a reasonable explanatory power given the complexity of cleft risk. In such a model, one can calculate how individual-level risk changes with different values of these phenotypes. This example highlights the capacity of improved subphenotypic characterization for predicting NSCL/P risk. Certainly, reliable risk estimation requires development of these models in larger data sets. In addition, our study presents suggestive evidence that genes involved in lip and palate formation also contribute to facial features that are part of the overall phenotypic spectrum of orofacial clefting and such features are more commonly present in individuals who carry a genetic risk for oral clefts. Even though most of our findings on phenotype differences or genetic associations do not surpass a Bonferroni correction for multiple testing, the results as a whole, including the significant findings after this correction and the multiple suggestive findings consistent with previous findings and knowledge of biological mechanisms, lend support to our hypothesis of a genetically influenced wide phenotypic spectrum of NSCL/P and to the value of our research approach. Therefore, future studies should assign these genetic pathways high priority.

Of course, the limitation of small sample size and power point to the need for larger sample sizes in the future. To further increase our understanding of the phenotypic diversity in NSCL/P and underlying etiologies, future large consortium studies combining multiple sources of samples and extensive genetic data sets including genome-wide association study (GWAS) data and any sequencing data will be needed. Such studies will further enable the heterogeneity in subphenotyping variation and genetic associations to be explored not only by age/gender, which we explore in this study, but also by cleft type (i.e. cleft lip only vs. cleft lip and palate), a potentially important modifier that we were unable to examine due to the small sample size. Fortunately, such collaborative efforts are underway and will eventually offer an opportunity to test our findings on larger data sets and expand our research question to many more genetic pathways. Such studies could bring tremendous value for the improvement of the prediction of risk for and diagnosis of NSCL/P and for the design of novel therapies that can improve surgical outcomes in patients with craniofacial conditions.

Acknowledgements

References

Arosarena OA. Cleft lip and palate. Otolaryngol Clin North Am. 2007; 40:27, 60, vi. [PubMed: 17346560]

Bamforth JS, Hughes IA, Lazarus JH, et al. Congenital hypothyroidism, spiky hair, and cleft palate. J Med Genet. 1989; 26:49–51. [PubMed: 2918525]

Beaty TH, Murray JC, Marazita ML, et al. A genome-wide association study of cleft lip with and without cleft palate identifies risk variants near MAFB and ABCA4. Nat Genet. 2010; 42:525–529. [PubMed: 20436469]

Bei M, Maas R. FGFs and BMP4 induce both Msx1-independent and Msx1-dependent signaling pathways in early tooth development. Development. 1998; 125:4325–4333. [PubMed: 9753686]

Birnbaum S, Ludwig KU, Reutter H, et al. Key susceptibility locus for nonsyndromic cleft lip with or without cleft palate on chromosome 8q24. Nat Genet. 2009; 41:473–477. [PubMed: 19270707]

Bishara SE, Jakobsen JR, Krause JC, et al. Cephalometric comparisons of individuals from India and Mexico with unoperated cleft lip and palate. Cleft Palate J. 1986; 23:116–125. [PubMed: 3457658]

Bock MT, Bowman AW. On the measurement and analysis of asymmetry with applications to facial modelling. J Roy Stat Soc: Ser C (Appl Stat). 2006; 55:77–91.

Boehringer S, van der Lijn F, Liu F, et al. Genetic determination of human facial morphology: links between cleft-lips and normal variation. Eur J Hum Genet. 2011; 19:1192–1197. [PubMed: 21694738]

van den Boogaard MJ, Dorland M, Beemer FA, et al. MSX1 mutation is associated with orofacial clefting and tooth agenesis in humans. Nat Genet. 2000; 24:342–343. [PubMed: 10742093]

Boorman CJ, Shimeld SM. Pitx homeobox genes in Ciona and amphioxus show left–right asymmetry is a conserved chordate character and define the ascidian adenohypophysis. Evol Dev. 2002; 4:354–365. [PubMed: 12356265]

Brugmann SA, Powder KE, Young NM, et al. Comparative gene expression analysis of avian embryonic facial structures reveals new candidates for human craniofacial disorders. Hum Mol Genet. 2010; 19:920–930. [PubMed: 20015954]

Chevrier C, Perret C, Bahuau M, et al. Interaction between the ADH1C polymorphism and maternal alcohol intake in the risk of nonsyndromic oral clefts: an evaluation of the contribution of child and maternal genotypes. Birth Defects Res A Clin Mol Teratol. 2005; 73:114–122. [PubMed: 15602753]

Dahl E, Koseki H, Balling R. Pax genes and organogenesis. BioEssays. 1997; 19:755–765. [PubMed: 9297966]

Davis NM, Kurpios NA, Sun X, et al. The chirality of gut rotation derives from left-right asymmetric changes in the architecture of the dorsal mesentery. Dev Cell. 2008; 15:134–145. [PubMed: 18606147]

Dixon MJ, Marazita ML, Beaty TH, et al. Cleft lip and palate: understanding genetic and environmental influences. Nat Rev Genet. 2011; 12:167–178. [PubMed: 21331089]

Gage PJ, Suh H, Camper SA. Dosage requirement of Pitx2 for development of multiple organs. Development. 1999; 126:4643–4651. [PubMed: 10498698]

Grant SF, Wang K, Zhang H, et al. A genome-wide association study identifies a locus for nonsyndromic cleft lip with or without cleft palate on 8q24. J Pediatr. 2009; 155:909–913. [PubMed: 19656524]

Hamada H, Meno C, Watanabe D, et al. Establishment of vertebrate left-right asymmetry. Nat Rev Genet. 2002; 3:103–113. [PubMed: 11836504]

Hintze, J. NCSS, PASS, and GESS. Kaysville, UT: NCSS; 2006.

Incrapera AK, Kau CH, English JD, et al. Soft tissue images from cephalograms compared with those from a 3D surface acquisition system. Angle Orthod. 2010; 80:58–64. [PubMed: 19852641]

Ingraham CR, Kinoshita A, Kondo S, et al. Abnormal skin, limb and craniofacial morphogenesis in mice deficient for interferon regulatory factor 6 (Irf6). Nat Genet. 2006; 38:1335–1340. [PubMed: 17041601]

Johnson W, Gangestad SW, Segal NL, et al. Heritability of fluctuating asymmetry in a human twin sample: the effect of trait aggregation. Am J Hum Biol. 2008; 20:651–658. [PubMed: 18449924]

Kaartinen V, Voncken JW, Shuler C, et al. Abnormal lung development and cleft palate in mice lacking TGF-beta 3 indicates defects of epithelial-mesenchymal interaction. Nat Genet. 1995; 11:415–421. [PubMed: 7493022]

Kirschner RE, LaRossa D. Cleft lip and palate. Otolaryngol Clin North Am. 2000; 33:1191, 215, v–vi. [PubMed: 11449783]

Klingenberg CP. MorphoJ: an integrated software package for geometric morphometrics. Mol Ecol Resour. 2011; 11:353–357. [PubMed: 21429143]

Klingenberg CP, Monteiro LR. Distances and directions in multidimensional shape spaces: implications for morphometric applications. Syst Biol. 2005; 54:678–688. [PubMed: 16126663]

Klingenberg CP, Nijhout HF. Genetics of fluctuating asymmetry: a developmental model of developmental instability. Evolution. 1999; 53:358–375.

Klingenberg CP, Leamy LJ, Routman EJ, et al. Genetic architecture of mandible shape in mice: effects of quantitative trait loci analyzed by geometric morphometrics. Genetics. 2001; 157:785–802. [PubMed: 11156997]

Klingenberg CP, Barluenga M, Meyer A. Shape analysis of symmetric structures: quantifying variation among individuals and asymmetry. Evolution. 2002; 56:1909–1920. [PubMed: 12449478]

Klingenberg CP, Wetherill L, Rogers J, et al. Prenatal alcohol exposure alters the patterns of facial asymmetry. Alcohol. 2010; 44:649–657. [PubMed: 20060678]

Kurpios NA, Ibañes M, Davis NM, et al. The direction of gut looping is established by changes in the extracellular matrix and in cell: cell adhesion. Proc Natl Acad Sci USA. 2008; 105:8499–8506. [PubMed: 18574143]

Landis JR, Koch GG. The measurement of observer agreement for categorical data. Biometrics. 1977; 33:159–174. [PubMed: 843571]

Leamy L. Heritability of directional and fluctuating asymmetry for mandibular characters in random-bred mice. J Evol Biol. 1999; 12:146–155.

Leamy LJ, Pomp D, Eisen EJ, et al. Quantitative trait loci for directional but not fluctuating asymmetry of mandible characters in mice. Genet Res. 2000; 76:27–40. [PubMed: 11006632]

Leamy LJ, Routman EJ, Cheverud JM. An epistatic genetic basis for fluctuating asymmetry of mandible size in mice. Evolution. 2002; 56:642–653. [PubMed: 11989692]

Leamy LJ, Workman MS, Routman EJ, et al. An epistatic genetic basis for fluctuating asymmetry of tooth size and shape in mice. Heredity. 2005; 94:316–325. [PubMed: 15674385]

Leslie EJ, Mansilla MA, Biggs LC, et al. Expression and mutation analyses implicate ARHGAP29 as the etiologic gene for the cleft lip with or without cleft palate locus identified by genome-wide association on chromosome 1p22. Birth Defects Res A Clin Mol Teratol. 2012; 94:934–942. [PubMed: 23008150]

Liao YF, Mars M. Long-term effects of clefts on craniofacial morphology in patients with unilateral cleft lip and palate. Cleft Palate Craniofac J. 2005; 42:601–609. [PubMed: 16241171]

Lidral AC, Romitti PA, Basart AM, et al. Association of MSX1 and TGFB3 with nonsyndromic clefting in humans. Am J Hum Genet. 1998; 63:557–568. [PubMed: 9683588]

Lin CR, Kioussi C, O'Connell S, et al. Pitx2 regulates lung asymmetry, cardiac positioning and pituitary and tooth morphogenesis. Nature. 1999; 401:279–282. [PubMed: 10499586]

Liu F, van der Lijn F, Schurmann C, et al. A genome-wide association study identifies five loci influencing facial morphology in Europeans. PLoS Genet. 2012; 8:e1002932. [PubMed: 23028347]

Lu MF, Pressman C, Dyer R, et al. Function of Rieger syndrome gene in left-right asymmetry and craniofacial development. Nature. 1999; 401:276–278. [PubMed: 10499585]

Lubbers HT, Medinger L, Kruse A, et al. Precision and accuracy of the 3dMD photogrammetric system in craniomaxillofacial application. J Craniofac Surg. 2010; 21:763–767. [PubMed: 20485043]

Ludwig KU, Mangold E, Herms S, et al. Genome-wide meta-analyses of nonsyndromic cleft lip with or without cleft palate identify six new risk loci. Nat Genet. 2012; 44:968–971. [PubMed: 22863734]

Mangold E, Ludwig KU, Birnbaum S, et al. Genome-wide association study identifies two susceptibility loci for nonsyndromic cleft lip with or without cleft palate. Nat Genet. 2010; 42:24–26. [PubMed: 20023658]

Mansouri A, Stoykova A, Torres M, et al. Dysgenesis of cephalic neural crest derivatives in Pax7$^{-/-}$ mutant mice. Development. 1996; 122:831–838. [PubMed: 8631261]

Marazita ML. The evolution of human genetic studies of cleft lip and cleft palate. Annu Rev Genomics Hum Genet. 2012; 13:263–283. [PubMed: 22703175]

Mardia KV, Bookstein FL, Moreton IJ. Statistical assessment of bilateral symmetry of shapes. Biometrika. 2000; 87:285–300.

Maulina I, Urtane I, Jakobsone G. The craniofacial morphology of the parents of children with cleft lip and/or palate: a review of cephalometric studies. Stomatologija. 2006; 8:16–20. [PubMed: 16687910]

McIntyre GT, Mossey PA. Asymmetry of the parental craniofacial skeleton in orofacial clefting. J Orthod. 2002; 29:299–305. discussion 278–9. [PubMed: 12444271]

McIntyre GT, Mossey PA. Asymmetry of the craniofacial skeleton in the parents of children with a cleft lip, with or without a cleft palate, or an isolated cleft palate. Eur J Orthod. 2010; 32:177–185. [PubMed: 20083809]

Menezes R, Vieira AR. Dental anomalies as part of the cleft spectrum. Cleft Palate Craniofac J. 2008; 45:414–419. [PubMed: 18616370]

Meno C, Ito Y, Saijoh Y, et al. Two closely-related left–right asymmetrically expressed genes, lefty-1 and lefty-2: their distinct expression domains, chromosomal linkage and direct neuralizing activity in Xenopus embryos. Genes Cells. 1997; 2:513–524. [PubMed: 9348041]

Mitsiadis TA, Angeli I, James C, et al. Role of Islet1 in the patterning of murine dentition. Development. 2003; 130:4451–4460. [PubMed: 12900460]

Modesto A, Moreno LM, Krahn K, et al. MSX1 and orofacial clefting with and without tooth agenesis. J Dent Res. 2006; 85:542–546. [PubMed: 16723652]

Moreno LM, Mansilla MA, Bullard SA, et al. FOXE1 association with both isolated cleft lip with or without cleft palate, and isolated cleft palate. Hum Mol Genet. 2009; 18:4879–4896. [PubMed: 19779022]

Mossey PA, Little J, Munger RG, et al. Cleft lip and palate. Lancet. 2009; 374:1773–1785. [PubMed: 19747722]

Murray SA, Gridley T. Snail family genes are required for left-right asymmetry determination, but not neural crest formation, in mice. Proc Natl Acad Sci USA. 2006; 103:10300–10304. [PubMed: 16801545]

Murray SA, Oram KF, Gridley T. Multiple functions of Snail family genes during palate development in mice. Development. 2007; 134:1789–1797. [PubMed: 17376812]

Neiswanger K, Cooper ME, Weinberg SM, et al. Cleft lip with or without cleft palate and dermatoglyphic asymmetry: evaluation of a Chinese population. Orthod Craniofac Res. 2002; 5:140–146. [PubMed: 12194662]

Neiswanger K, Cooper ME, Liu YE, et al. Bilateral asymmetry in Chinese families with cleft lip with or without cleft palate. Cleft Palate Craniofac J. 2005; 42:192–196. [PubMed: 15748111]

Neiswanger K, Chirigos KW, Klotz CM, et al. Whorl patterns on the lower lip are associated with nonsyndromic cleft lip with or without cleft palate. Am J Med Genet A. 2009; 149A:2673–2679. [PubMed: 19921634]

Nystrom M, Ranta R. Dental age and asymmetry in the formation of mandibular teeth in twins concordant or discordant for oral clefts. Scand J Dent Res. 1988; 96:393–398. [PubMed: 3201110]

Otero L, Bermudez L, Lizarraga K, et al. A comparative study of facial asymmetry in Philippine, Colombian, and Ethiopian families with nonsyndromic cleft lip palate. Plast Surg Int. 2012; 2012:580769. [PubMed: 23150817]

Palmer, AR. Fluctuating asymmetry analyses: a primer. In: Markow, TA., editor. Developmental Instability: Its Origins and Evolutionary Implications. Dordrecht, Netherlands: Kluwer; 1994. p. 335-364.

Palmer AR, Strobeck C. Fluctuating asymmetry as a measure of developmental stability: implications of non-normal distributions and power of statistical tests. Acta Zool Fenn. 1992; 191:57–72.

Paznekas WA, Okajima K, Schertzer M, et al. Genomic organization, expression, and chromosome location of the human SNAIL gene (SNAI1) and a related processed pseudo-gene (SNAI1P). Genomics. 1999; 62:42–49. [PubMed: 10585766]

Rahimov F, Marazita ML, Visel A, et al. Disruption of an AP-2alpha binding site in an IRF6 enhancer is associated with cleft lip. Nat Genet. 2008; 40:1341–1347. [PubMed: 18836445]

Riley BM, Murray JC. Sequence evaluation of FGF and FGFR gene conserved non-coding elements in non-syndromic cleft lip and palate cases. Am J Med Genet A. 2007; 143A:3228–3234. [PubMed: 17963255]

Riley BM, Mansilla MA, Ma J, et al. Impaired FGF signaling contributes to cleft lip and palate. Proc Natl Acad Sci U S A. 2007; 104:4512–4517. [PubMed: 17360555]

Satokata I, Maas R. Msx1 deficient mice exhibit cleft palate and abnormalities of craniofacial and tooth development. Nat Genet. 1994; 6:348–356. [PubMed: 7914451]

Seager DC, Kau CH, English JD, et al. Facial morphologies of an adult Egyptian population and an adult Houstonian white population compared using 3D imaging. Angle Orthod. 2009; 79:991–999. [PubMed: 19705950]

Semina EV, Reiter R, Leysens NJ, et al. Cloning and characterization of a novel bicoid-related homeobox transcription factor gene, RIEG, involved in Rieger syndrome. Nat Genet. 1996; 14:392–399. [PubMed: 8944018]

da Silva Filho OG, da Castro Machado FM, da Andrade AC, et al. Upper dental arch morphology of adult unoperated complete bilateral cleft lip and palate. Am J Orthod Dentofac Orthop. 1998; 114:154–161.

Slayton RL, Williams L, Murray JC, et al. Genetic association studies of cleft lip and/or palate with hypodontia outside the cleft region. Cleft Palate Craniofac J. 2003; 40:274–279. [PubMed: 12733956]

Sofaer JA. Human tooth-size asymmetry in cleft lip with or without cleft palate. Arch Oral Biol. 1979; 24:141–146. [PubMed: 299139]

StataCorp. Stata Statistical Software: Release 12. College Station, TX: StataCorp LP; 2011. URL: http://www.stata.com/.

Sull JW, Liang KY, Hetmanski JB, et al. Maternal transmission effects of the PAX genes among cleft case-parent trios from four populations. Eur J Hum Genet. 2009; 17:831–839. [PubMed: 19142206]

Suzuki S, Marazita ML, Cooper ME, et al. Mutations in BMP4 are associated with subepithelial, microform, and overt cleft lip. Am J Hum Genet. 2009; 84:406–411. [PubMed: 19249007]

Tzahor E. Heart and craniofacial muscle development: a new developmental theme of distinct myogenic fields. Dev Biol. 2009; 327:273–279. [PubMed: 19162003]

Valen LV. A study of fluctuating asymmetry. Evolution. 1962; 16:125–142.

Venza I, Visalli M, Parrillo L, et al. MSX1 and TGF-β3 are novel target genes functionally regulated by FOXE1. Hum Mol Genet. 2011; 20:1016–1025. [PubMed: 21177256]

Vieira AR, Modesto A, Meira R, et al. Interferon regulatory factor 6 (IRF6) and fibroblast growth factor receptor 1 (FGFR1) contribute to human tooth agenesis. Am J Med Genet A. 2007; 143:538–545. [PubMed: 17318851]

Wehby GL, Cassell CH. The impact of orofacial clefts on quality of life and healthcare use and costs. Oral Dis. 2010; 16:3–10. [PubMed: 19656316]

Weinberg SM, Neiswanger K, Martin RA, et al. The Pittsburgh Oral-Facial Cleft study: expanding the cleft phenotype. Background and justification. Cleft Palate Craniofac J. 2006; 43:7–20. [PubMed: 16405378]

Weinberg SM, Neiswanger K, Richtsmeier JT, et al. Three-dimensional morphometric analysis of craniofacial shape in the unaffected relatives of individuals with nonsyndromic orofacial clefts: a possible marker for genetic susceptibility. Am J Med Genet A. 2008a; 146A:409–420. [PubMed: 18203157]

Weinberg SM, Brandon CA, McHenry TH, et al. Rethinking isolated cleft palate: evidence of occult lip defects in a subset of cases. Am J Med Genet A. 2008b; 146A:1670–1675. [PubMed: 18536047]

Weinberg SM, Naidoo SD, Bardi KM, et al. Face shape of unaffected parents with cleft affected offspring: combining three-dimensional surface imaging and geometric morphometrics. Orthod Craniofac Res. 2009; 12:271–281. [PubMed: 19840279]

Werner SP, Harris EF. Odontometrics of the permanent teeth in cleft lip and palate: systemic size reduction and amplified asymmetry. Cleft Palate J. 1989; 26:36–41. [PubMed: 2917415]

Wooldridge, JM. Econometric Analysis of Cross Section and Panel Data. Cambridge, MA: The MIT press; 2002.

Wu T, Liang KY, Hetmanski JB, et al. Evidence of gene–environment interaction for the IRF6 gene and maternal multivitamin supplementation in controlling the risk of cleft lip with/without cleft palate. Hum Genet. 2010; 128:401–410. [PubMed: 20652317]

Yoon YJ, Perkiomaki MR, Tallents RH, et al. Association of nasomaxillary asymmetry in children with unilateral cleft lip and palate and their parents. Cleft Palate Craniofac J. 2003; 40:493–497. [PubMed: 12943439]

Yuan S, Schoenwolf GC. Islet-1 marks the early heart rudiments and is asymmetrically expressed during early rotation of the foregut in the chick embryo. Anat Rec. 2000; 260:204–207. [PubMed: 10993956]

Zucchero TM, Cooper ME, Maher BS, et al. Interferon regulatory factor 6 (IRF6) gene variants and the risk of isolated cleft lip or palate. N Engl J Med. 2004; 351:769–780. [PubMed: 15317890]
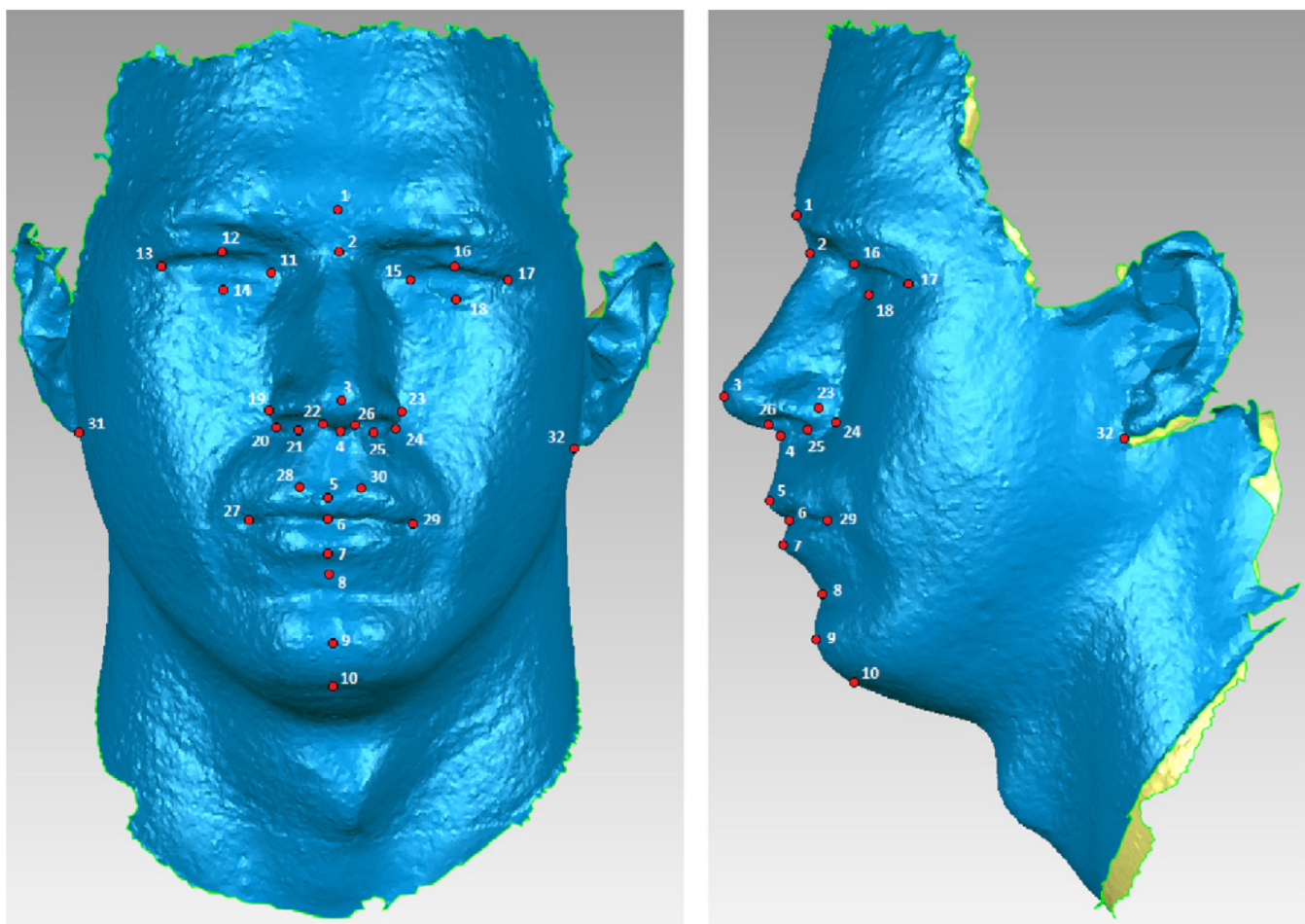
Fig. 1.
A graphical representation of the location of all 32 coordinate landmarks. For a complete list and descriptions, refer to Table 4.
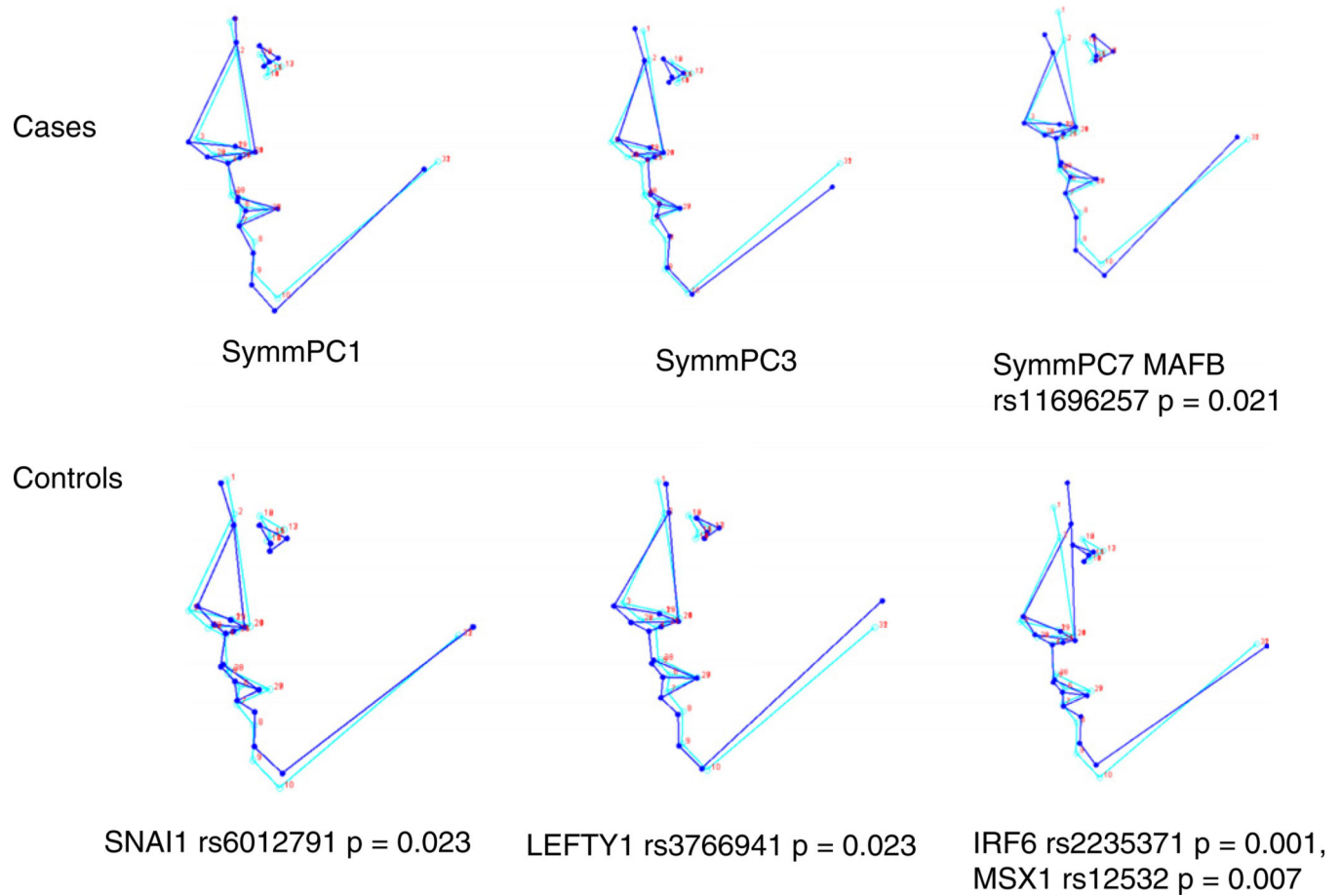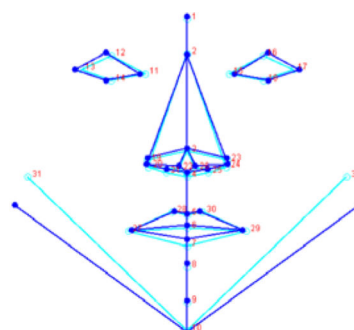
Fig. 2.

Lateral view of the three components of facial shape symmetric variation SymmPC1, SymmPC3 and SymmPC7 found to differ significantly ($P < 0.05$) between cases and controls in the pooled sample. From this figure on, light blue represents the average facial shape configuration within each component and dark blue represents a configuration with an arbitrary positive or negative PC score for each component shown. To facilitate case–control shape comparisons, positive and negative configurations were displayed so that those representing cases are shown on the top panel and controls in the bottom panel. Also shown are genes and loci that correlated with specific shape components. The position of the gene in each diagram indicates that more copies of a rare allele of the gene in an individual's genotype are correlated with that specific facial shape.
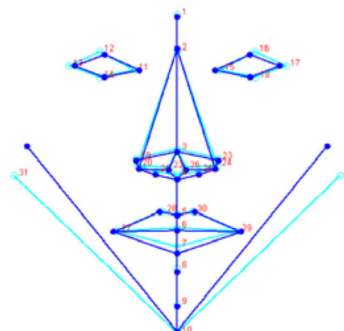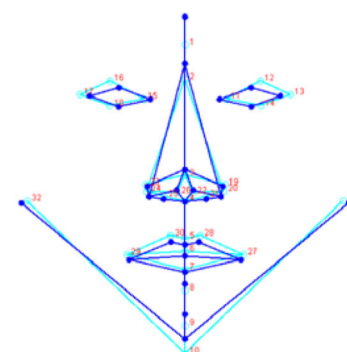
Cases
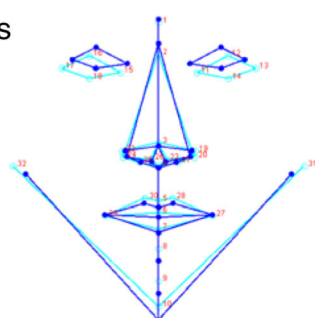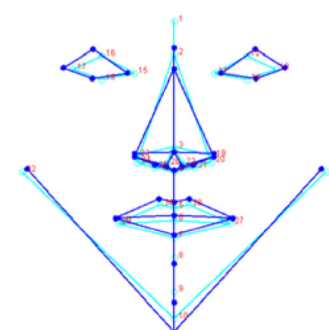
SymmPC1 SymmPC3 SymmPC7 MAFB
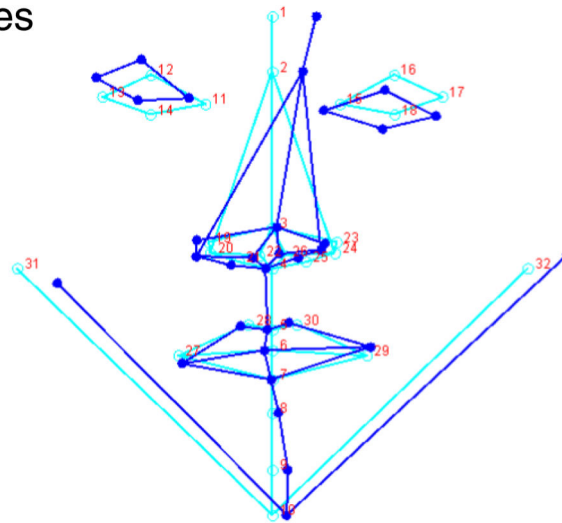rs11696257 p = 0.021

Controls
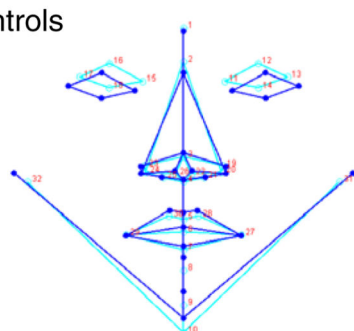
SNAI1 rs6012791
p = 0.023

LEFTY1 rs3766941
p = 0.023

IRF6 rs2235371 p = 0.001,
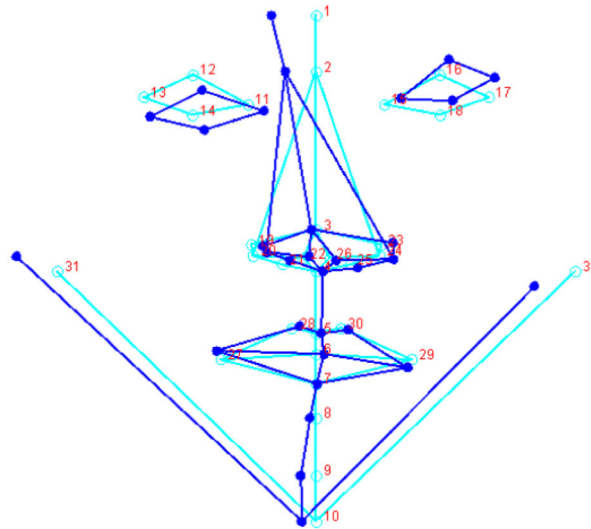MSX1 rs12532 p = 0.007

Fig. 3.
Frontal view of the three components of facial shape symmetric variation SymmPC1,
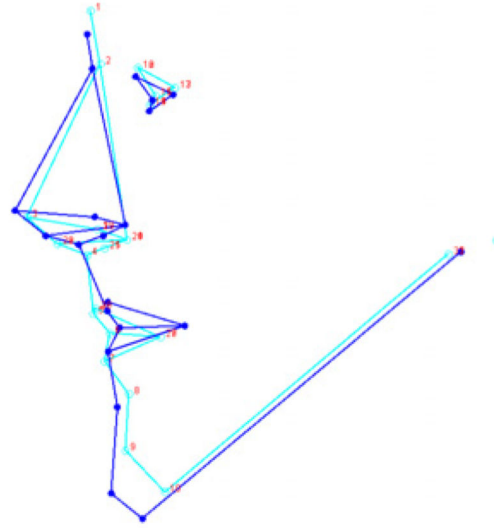SymmPC3 and SymmPC7 found to differ between cases and controls in the pooled sample.
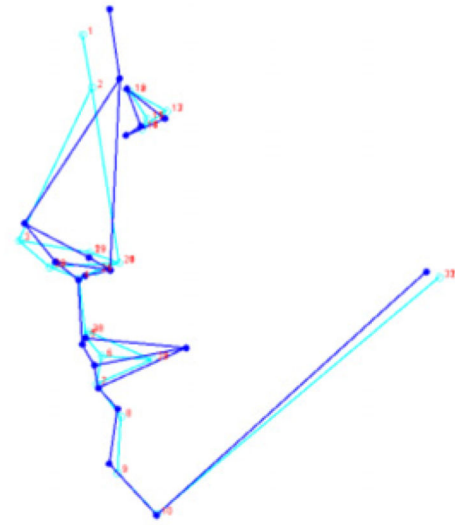
Fig. 4.
Frontal view of the one component of facial shape asymmetric variation AsymmPC4 found to differ significantly ($P < 0.05$) between cases and controls in the pooled sample.
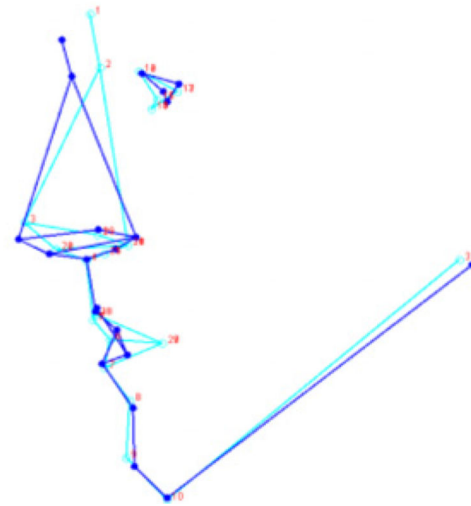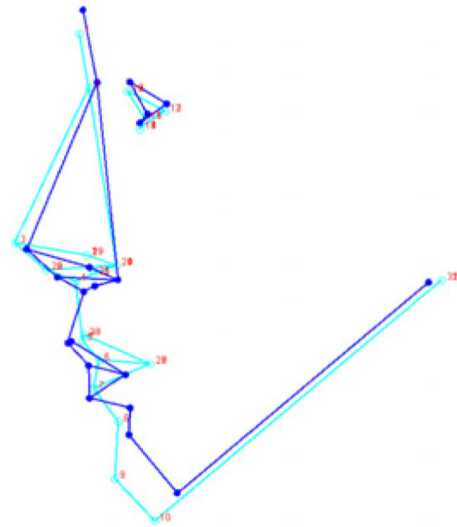
Cases

SymmPC6   SymmPC10 *ABCA4-ARHGAP29*
p = 0.0005

Controls
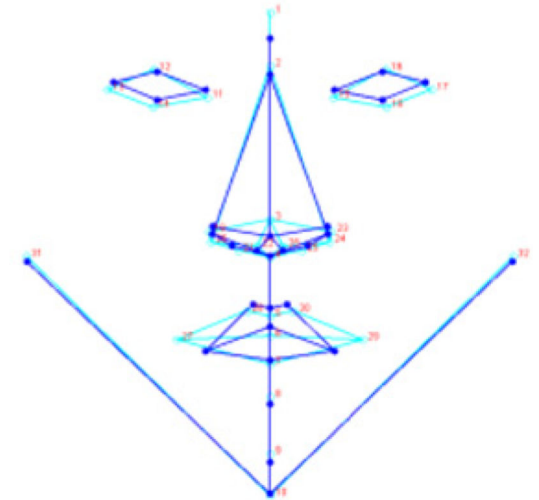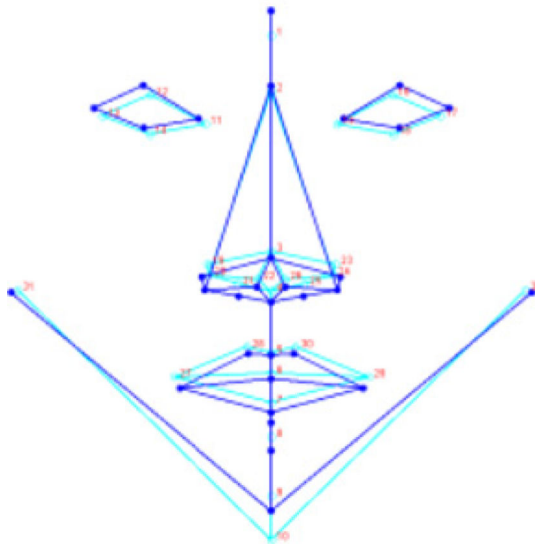
Fig. 5.
Lateral view of the components of facial shape symmetric variation found to differ between cases (top) and controls (bottom) in the female adult sample.

Fig. 6.
Frontal view of the components of facial shape symmetric variation found to differ between cases (top) and controls (bottom) in the female adult sample.
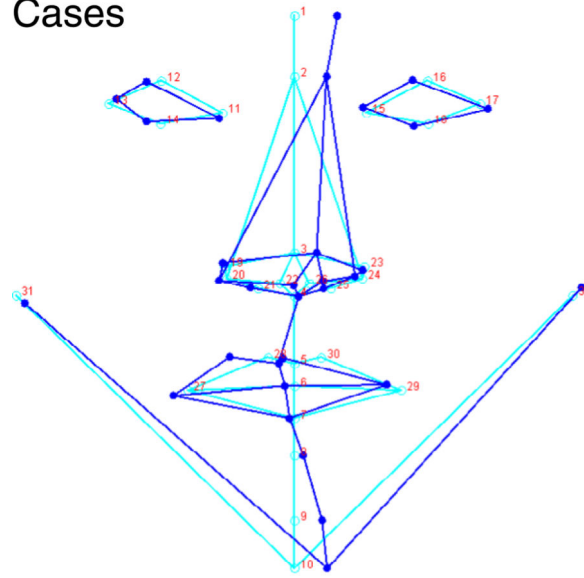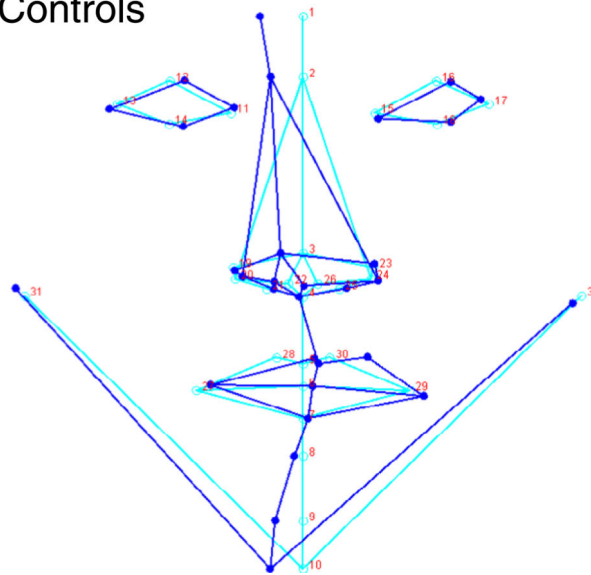
Fig. 7.
Components of facial shape asymmetric variation found to differ between cases (top) and controls (bottom) in the adult female samples.

Fig. 8.
Lateral and frontal view of the component SymmPC5 of facial shape symmetric variation found to differ between cases and controls in the male sub adult sample.

Cases

SymmPC2
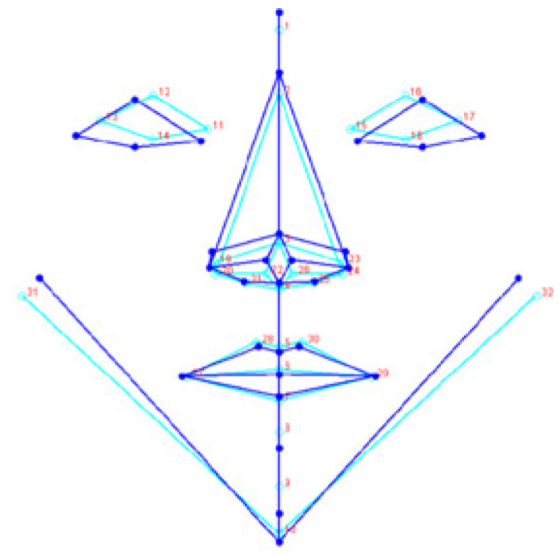
SymmPC9

Controls

LEFTY1 p = 0.037
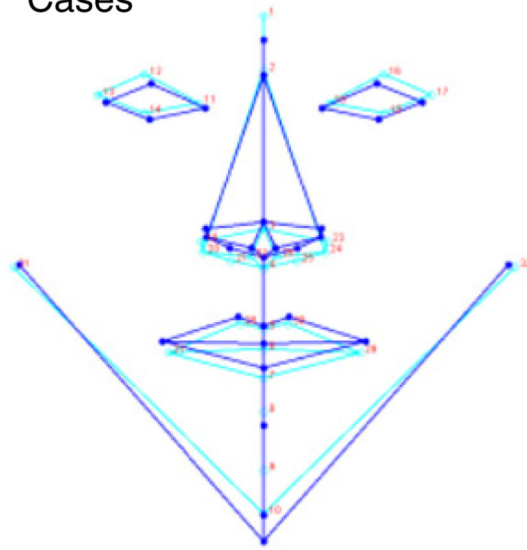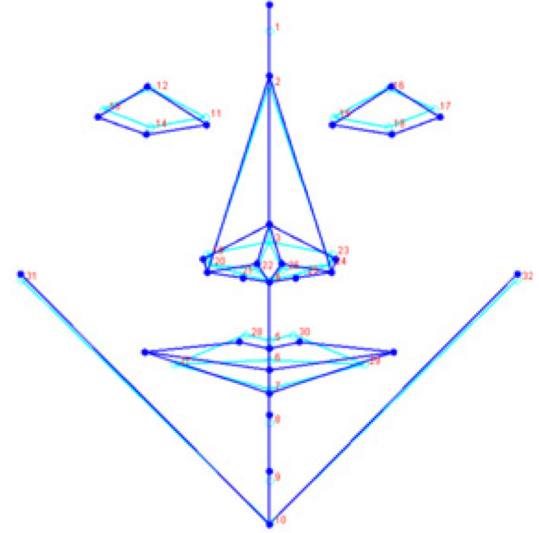
Fig. 9.
Lateral view of the components of facial shape symmetric variation found to differ between cases (top) and controls (bottom) in the female subadult sample.
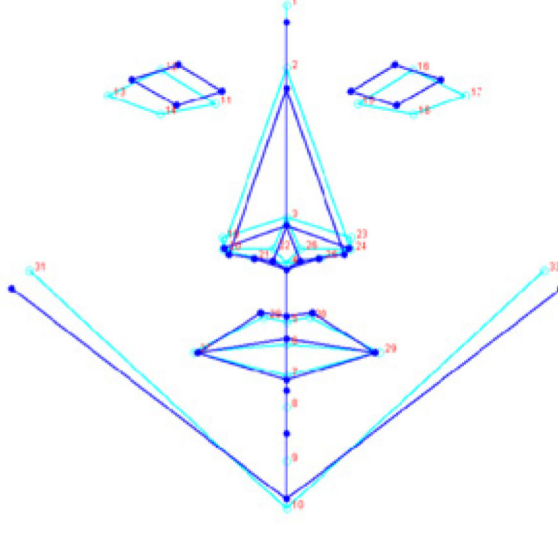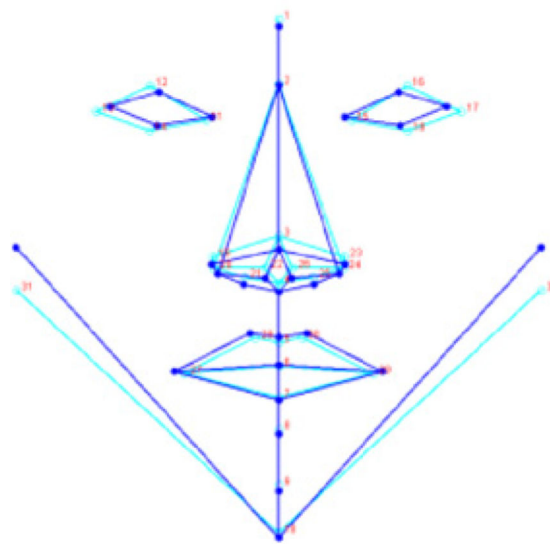
Fig. 10.
Frontal view of the components of facial shape symmetric variation found to differ between cases (top) and controls (bottom) in the female sub adult sample.
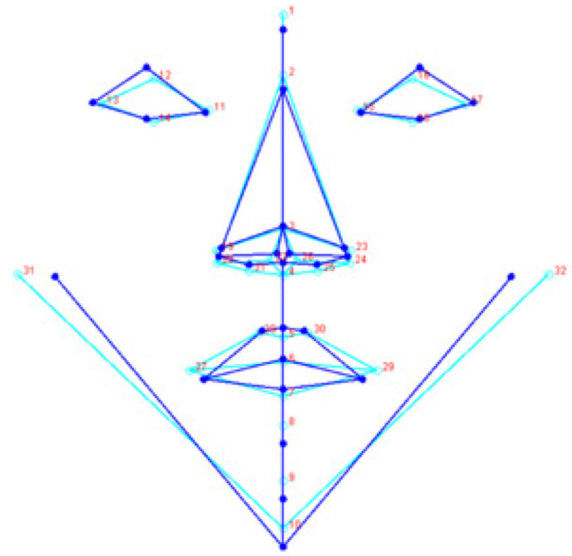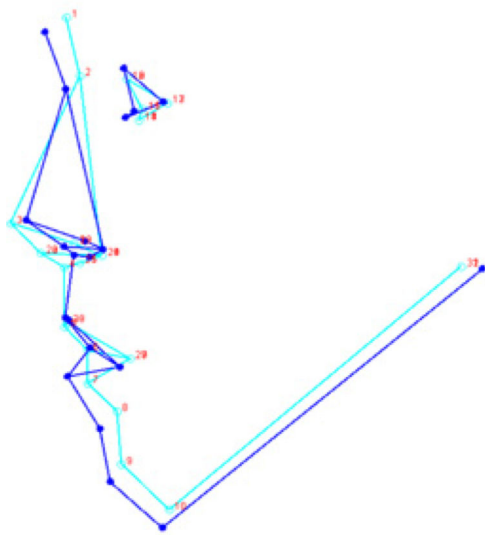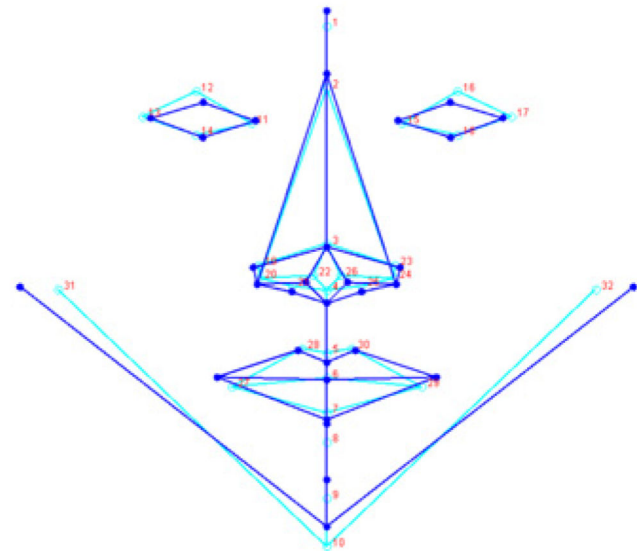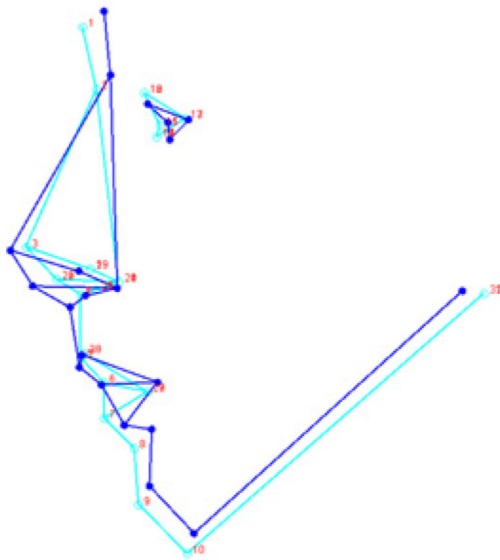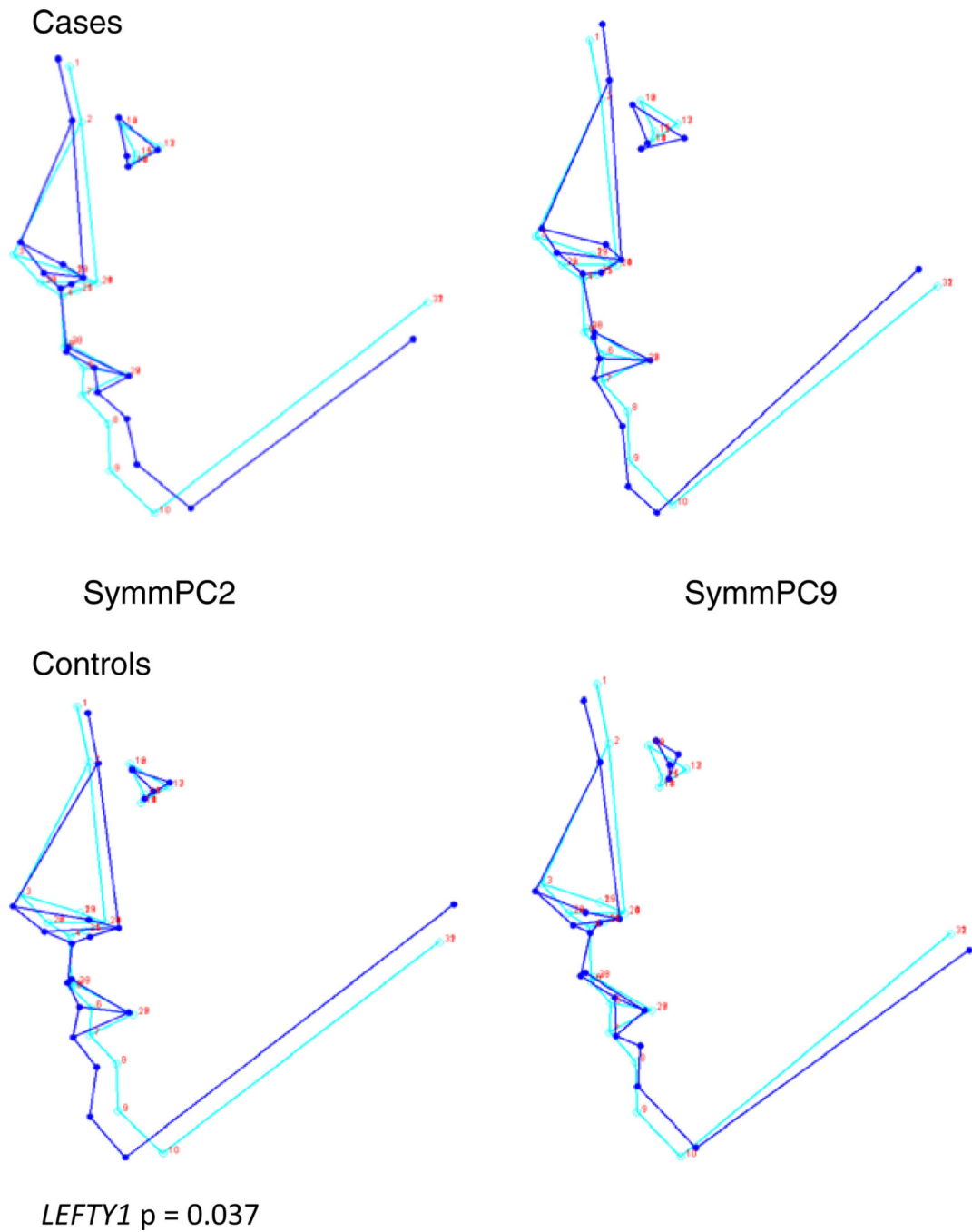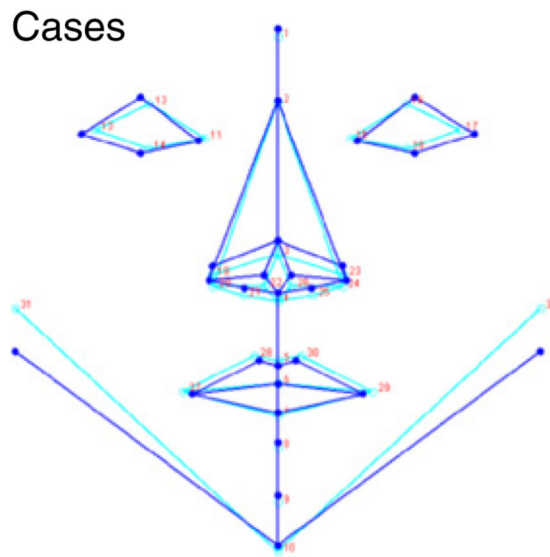
Table 1

Listing and description of clefting and craniofacial candidate genes genotyped for the present study.

Gene	Selective[*] references reporting association with NSCL/P	Gene expression pattern and/or craniofacial anomalies associated	References
PAX7	Sull et al. (2009) and Ludwig et al. (2012)	PAX 7 is expressed in craniofacial neural crest derivatives and knockout mice exhibit malformations in the maxilla and nose	Mansouri et al. (1996)
ABCA4-ARHGAP29	Beaty et al. (2010) and Leslie et al. (2012)	ARHGAP29 is expressed in the medial and lateral nasal processes, maxilla, mandible and secondary palatal shelves	Leslie et al. (2012)
IRF6	Rahimov et al. (2008)	IRF6 knockouts present with shorter and rounded snouts and jaws	Ingraham et al. (2006)
MSX1	Lidral et al. (1998)	MSX1 null mice present with anomalies of the frontal and nasal bone, reduced overall length of the mandible, deficient alveolar bone, abnormal dental development and cleft palate	Satokata & Maas (1994)
8q24_rs987525	Birnbaum et al. (2009) and Grant et al. (2009)	rs987525 was found associated with bizygomatic distance in a recent GWAS study	Boehringer et al. (2011)
FOXE1	Moreno et al. (2009)	Mutations in FOXE caused Bamforth–Lazarous syndrome in humans characterized by hypothyroidism, hair and craniofacial anomalies including cleft palate and ocular hypertelorism	Bamforth et al. (1989)
TGFB3	Lidral et al. (1998)	TGFB3 Null mice present with cleft palate. TGFB3 is differentially expressed in the different species of bird beaks and presumably playing a role in the morphogenesis of avian beaks	Kaartinen et al. (1995) and Brugmann et al. (2010)
MAFB	Beaty et al. (2010)	MAFB is expressed in the craniofacial ectoderm, palatal shelves and nasal septum	Beaty et al. (2010)

[*] Many other studies have reported association between these genes and NSCL/P (see review Dixon et al., 2011; Marazita, 2012).

Table 2

Listing and description of left–right (L/R) body patterning candidate genes genotyped for the present study.

Gene	Role in L/R body patterning	References	Craniofacial expression and/or craniofacial anomalies associated	References
LFFTY1	Member of the TGFB family that functions as an antagonist of the Nodal signaling which is essential or the L/R patterning of the embryo. *Lefty1* is expressed on the left side of the prospective floor plate and acts as the anterior midline barrier to signals that determine leftness. *Lefty1* null mice in which Nodal, *Lefty2* and *Pilx2* are expressed bilaterally in the lateral plate mesoderm (LPM) develop left isomerism (both sides develop left side characteristics)	Hamada et al. (2002)		
LFFTY2	Also a member of the TGFB family of proteins. Expression of *Lefty2* is induced by nodal also on the left side of the LPM. *Lefty2* is not a left-side determinant but a regular of the Nodal action. *Lefty2* mutant mice have a prolonged expression of Nodal and also develop left isomerism	Hamada et al. (2002)		
PITX2	Transcription factor important in asymmetric morphogenesis in response to Nodal. It is expressed in the left side of the LPM and persists longer than Nodal and *Lefty2*. *Pitx2* is also expressed in the primordia of asymmetric organs and midgut during development. *Pitx2* null embryos develop cardiac defects and right pulmonary isomerism	Lu et al. (1999)	In mice, *Pitx2* is expressed in the epithelium of maxilla, mandible and the mesenchyme of the dental lamina. *Pitx2* null mice present defects in maxilla and mandible, cleft palate and arrested tooth development. Also, heterozygous mice for a Pitx2 null allele show malocclusion of teeth and marked asymmetry of the incisors. In humans, PITX2 mutations cause Reiger syndrome and patients present with maxillary hypoplasia, hypertelorism, telecanthus and dental anomalies of number and shape	Semina et al. (1996) and Lu et al. (1999; Gage et al. 1999)
ISL1	*ISL1* is a LIM homeodomain containing transcription regulator that participates in determining cell fate and thus is important in the embryogenesis of multiple organs and tissue types including the heart, pancreas and intestine. *Isl1* null mice exhibit large developmental anomalies and arrest early in development. *Isl1* and *Pitx2* are necessary and sufficient for the asymmetric morphological changes in the cells of the epithelium and mesenchyme of the dorsal mesentery which result in the midgut looping	Davis et al. (2008) and Kurpios et al. (2008)	*ISL1* cell lineage contributes to both cardiac and head muscle progenitors. In mice, *Isl1* is expressed in the medial splanchnic mesoderm of the distal region of the 1st branchial arch and also in the 2nd branchial arch derived muscles which control facial expression and to a lesser extend masticatory muscles such as masseter, pterygoid and temporalis and the mandibular adductor complex in the chick. In addition, *Isl1* is expressed in the oral epithelium of mice at E9 restricted to the distal region, which is the future site for incisor development. Subsequently, *Isl1* is expressed in epithelial cells during all stages of incisor development	Mitsiadis et al. (2003) and Tzahor (2009)
SNAI1	*Snai1* is a zinc finger transcriptional repressor important in epithelial to mesenchymal transitions that contribute to the formation of the mesoderm. *Snai1* null mice die shortly after birth due to defects in mesoderm formation. *Snai1* conditional knockouts present heart anomalies consistent with randomization in left–right specification. In addition, *Snai1* conditional embryos display bilateral expression of *Nodal*, *Lefty2* and *Pitx2* in the LPM and do not express *Lefty1* in the midline of the prospective floor plate. Thus *Snai1* functions downstream of the initial left–right symmetry-breaking event and regulates expression of laterality genes in the LPM	Murray & Gridley (2006)	*Snai1* is expressed throughout the palatal shelf mesenchyme with high levels along the medial edge epithelium (MEE). *Snai2* expression is more diffused but present throughout the palatal mesenchyme and epithelium. 50% of Snai2$^{-/-}$ have cleft palate, which is completely penetrant in Snai1$^{+/-}$ Snai2$^{-/-}$. The cleft palate in the Snai1$^{+/-}$ Snai2$^{-/-}$ is due to a fusion failure caused by abnormal cell death along the MEE and also a defect in periderm migration towards the oral and nasal epithelium. Neural crest specific Snai1 deletion in Snai2$^{-/-}$ mice present with multiple craniofacial defects including cleft palate caused by failure of the mandible to move forward similarly to Pierre Robin sequences. Also, mice presented with dome-shape skulls, shortened parietal bones and enlarged frontal foramen, confirming a role for Snai	Murray et al. (2007)

Gene	Role in L/R body patterning	References	Craniofacial expression and/or craniofacial anomalies associated	References
			genes in later development of cranial neural crest-derived structures	

Author Manuscript

Author Manuscript

Author Manuscript

Author Manuscript

Table 3

Sample size and composition.

Case group (unaffected relatives)	n	Mean age	Range	Controls (n)	Mean age	Range	P-value
Mothers	79	36.8	24–50	84	34.3	18–53	0.04
Fathers	40	39.7	29–54	40	37.0	18–70	0.22
Female Siblings	39	10.7	3–19	29	9.4	2–17	0.19
Male Siblings	30	11.2	3–24	41	9.3	0–16	0.07
Totals	188			194			

Table 4

A list of all 32 3D coordinate landmarks used in the present study with included descriptions. Refer to Fig. 1 for landmark locations.

No.	Landmark	Abbreviation	Description
1	Glabella	g	The most forward projecting point of the forehead in the midline of the supraorbital ridges
2	Nasion	n	The outer point of intersection between the nasion-sella line and the soft tissue profile (radiographic soft tissue nasion)
3	Pronasion	prn	The most prominent point on the tip of the nose when the head is placed in the eye–ear (horizontal) plane
4	Subnasale	sn	The point at which the nasal septum merges, in the midsagittal plane, with the upper lip
5	Labiale Superius	ls	The most prominent superior midline point of the vermillion border of the upper lip
6	Stomion	sto	The median point of the oral slit when the lips are closed
7	Labiale Inferius	li	The most prominent inferior midline point of the vermillion border of the lower lip
8	Sublabiale	sl	The deepest midline point on the labiomental fold, which determines the lower border of the lower lip or the upper border of the chin
9	Pogonion	pg	The craniometric point that is the most forward-projecting point on the anterior surface of the chin
10	Gnathion	gn	The lowest point on the anterior margin of the lower jaw in the midsagittal plane
11	Right Endocanthion	en	Inner corner of the right eye
12	Right Palpebrale Superius	ps	Highest point in the midportion of the free margin of right upper eyelid
13	Right Exocanthion	ex	Outer corner of the right eye
14	Right Palpebrale Inferius	pi	Lowest point in the midportion of the free margin of right lower eyelid
15	Left Endocanthion	en	Inner corner of the left eye
16	Left Palpebrale Superius	ps	Highest point in the midportion of the free margin of left upper eyelid
17	Left Exocanthion	ex	Outer corner of the left eye
18	Left Palpebrale Inferius	pi	Lowest point in the midportion of the free margin of left lower eyelid
19	Right Alare	al	Right-most lateral point on the alar contour
20	Right Alar Curvature Point	ac	The right-most lateral point on the curved baseline of each ala, indicating the facial insertion of the nasal wing base
21	Right Subalare	sbal	The right point at the lower limit of the alar base, where the alar base disappears into the skin of the upper lip
22	Right Columnella	c	Most anterior soft tissue point on right side of columnella
23	Left Alare	al	Left-most lateral point on the alar contour
24	Left Alar Curvature Point	ac	The left-most lateral point on the curved baseline of each ala, indicating the facial insertion of the nasal wing base
25	Left Subalare	sbal	The left point at the lower limit of each alar base, where the alar base disappears into the skin of the upper lip
26	Left Columnella	c	Most anterior soft tissue point on left side of columnella
27	Right Chelion	ch	Right point at the corner of the mouth on the labial commissure
28	Right Crista Philtri	cph	The right point on the elevated margin of the philtrum just above the vermillion line
29	Left Chelion	ch	Left point at the corner of the mouth on the labial commissure
30	Left Crista Philtri	cph	The left point on the elevated margin of the philtrum just above the vermillion line
31	Right Otobasion inferius	obi	Point of attachment of ear lobe to cheek on right side
32	Left Otobasion inferius	obi	Point of attachment of ear lobe to cheek on left side

Author Manuscript Author Manuscript Author Manuscript Author Manuscript

Table 5

Complete list of the 20 SNPs (and associated genes) analyzed.

CHR	Genes	SNPs	CHR	Genes	SNPs
1	*PAX7*	rs4920520	4	*MSX1*	rs12532
1	*PAX7*	rs766325	4	*PITX2**	rs1947187
1	*ABCA4-ARHGAP29*	rs560426	5	*ISL1**	rs3811911
1	*IRF6*	rs2235371	8	8q24	rs987525
1	*IRF6*	rs642961	9	*FOXE1*	rs3758249
1	*LEFTY1**	rs3766941	9	*FOXE1*	rs1443434
1	*LEFTY1**	rs360059	9	*FOXE1*	rs4460498
1	*LEFTY2**	rs2273405	14	*TGFB3*	rs1012861
1	*LEFTY2**	rs2493163	20	*MAFB*	rs11696257
4	*MSX1*	rs4075	20	*SNAI1**	rs6012791

SNPs were coded based on the number of copies of the rare allele (0–2) on a given genotype.

* Genes that are implicated in left–right body patterning.

Table 6

Significant results for case–control comparisons for principal component analyses of symmetric and asymmetric shape variation along with significant phenotype–genotype correlations for the pooled sample.

| Phenotype | Case vs. control comparisons | | | Phenotype–genotype correlations | | | Phenotype–genotype correlations including case–control status | | |
	Coeff.	P-value	Variation explained (%)	Gene (SNP)	Coeff.	P-value	Coeff.	P-value	% Explained
SymmPC1	0.0073632	0.015	19.6	SNAI1 (rs6012791)	−0.00542	0.023	0.0068438	0.023	7.08
SymmPC3	0.0062887	0.022	12.0	LEFTY1(rs3766941)	−0.01086	0.023	0.0066862	0.017	–
SymmPC7	0.0043094	0.011	3.6	IRF6 (rs2235371)	−0.0091	0.001	0.0040266	0.016	6.56
				MSX1 (rs12532)	−0.00307	0.007	0.0042756	0.012	0.78
				MAFB (rs11696257)	0.002449	0.021	0.004907	0.004	–
AsymmPC4	−0.0022799	0.000	6.6	MSX1 (rs12532)	0.000811	0.056	–	–	–

Table 7

Pooled sample (A) Procrustes shape ANOVA and (B) shape MANOVA.

Sample	Test	Effect	SS	MS	df	F	P (param.)
Pooled sample	Shape ANOVA	Status	0.01782156	0.0003637054	49	3.43	0.0001
		Indivdual	1.97160089	0.0001058862	18 620	10.60	0.0001
		Side	0.03538143	0.0008845358	40	88.58	0.0001
		Ind*Side	0.15217847	0.0000099855	15 240		

Sample	Test	Component	Effect	Pillai tr.	P (param.)
Pooled sample	Shape MANOVA	SymmC	Status	0.35	0.0001
		AsymmC	Status	0.16	0.0128
			Side	0.9o	0.0001

Table 8

Significant results for case–control comparisons of directional asymmetry (DA) along with significant genotype–phenotype correlation with DA. Results showed non-parametric *P* values after 10 000 permutations.

Discriminant function analysis for directional asymmetry (DA) measured in Procrustes distances (PD) and with the *T*-square (TS) statistic

Cases vs. controls DA in (PD)/(TS)	Controls vs. unilateral clefts DA in PD/TS	Controls vs. bilateral clefts DA in PD/TS	Unilateral vs. bilateral clefts DA in PD/TS
P value = 0.037/0.011	*P* value = 0.046/0.006	*P* value = 0.339/0.224	*P* value = 0.671/0.067

Discriminant function analyses for comparison of DA in Individuals with 0–2 copies of rare alleles on their genotypes

Genes	SNPs	0 vs 1		0 vs 2		1 vs 2	
		PD *P*-value	TS *P*-value	PD *P*-value	TS *P*-value	PS *P*-value	TS *P*-value
ABCA4-ARHGAP29	rs560426	0.403	0.445	0.071	0.509	0.005	0.366
LEFTY1	rs360059	0.027	0.250	0.234	0.637	0.329	0.071
LEFTY2	rs2273405	0.041	0.237	0.013	0.068	0.108	0.150
LEFTY2	rs2493163	0.035	0.306	0.016	0.054	0.100	0.163
MSX1	rs12532	0.970	0.975	0.103	0.007	0.124	0.141
SNAI1	rs6012791	0.569	0.656	0.011	0.024	0.005	0.184

Table 9

Significant results of case–control comparisons for symmetric and asymmetric shape along with centroid size and Mahalanobis FA in the stratified sample. Also significant phenotype–genotype correlations. Controls are used as the reference category.

Phenotype	Adult female					Subadult male					Subadult female				
	Coeff.	P-value	Gene (SNP)	Coeff.	P-value	Coeff.	P-value	Gene (SNP)	Coeff.	P-value	Coeff.	P-value	Gene (SNP)	Coeff.	P-value
SymmPC2	–	–	–	–	–	–	–	–	–	–	–0.0109	0.049	*LEFTY1* (rs360059)	0.011	0.0368
SymmPC5	–	–	–	–	–	0.0083	0.041	–	–	–	–	–	–	–	–
SymmPC6	–0.0048	0.038													
SymmPC9	–	–									0.0068	0.033	–	–	–
SymmPC10	–0.0044	0.009	*ABCA4-ARHGAP29* (rs560426)	–0.004	0.0005	–	–	–	–	–	–	–	–	–	–
AsymmPC5	–0.0019	0.018	*LEFTY1* (rs360059)	–0.0016	0.0417	–	–	–	–	–	–	–	–	–	–
Centroid Size	4.7143	0.002	–	–	–	–	–	–	–	–	–	–	–	–	–
Mahalanobis FA score	0.2567	0.038	–	–	–	–	–	–	–	–	–	–	–	–	–

Table 10

Procrustes (A) ANOVA and (B) MANOVA results for all subsamples in the study.

(A)

Subsample	Test	Effect	SS	MS	df	F	P (param.)
Adult males	Shape ANOVA	Status	0.00655663	0.0001338090	49	1.4	0.0334
		Individual	0.36403131	0.0000952463	3822	8.49	<0.0001
		Side	0.00688408	0.0001721020	40	15.34	<0.0001
		Ind*Side	0.03545659	0.0000112204	3160	N/A	N/A
Adult females	Shape ANOVA	Status	0.01208387	0.0002466100	49	2.6	<0.0001
		Individual	0.74911382	0.0000949568	7889	9.51	<0.0001
		Side	0.01412266	0.0003530660	40	35.37	<0.0001
		Ind*Side	0.06469278	0.0000099835	6480	N/A	N/A
Subadult males	Shape ANOVA	Status	0.00487544	0.0000994989	49	1.03	0.4145
		Individual	0.32632592	0.0000965176	3381	11.3	<0.0001
		Side	0.00919705	0.0002299260	40	26.92	<0.0001
		Ind*Side	0.02391626	0.0000085415	2800	N/A	N/A
Subadult females	Shape ANOVA	Status	0.00654781	0.0001336290	49	1.54	0.0093
		Individual	0.28010783	0.0000866134	3234	8.94	<0.0001
		Side	0.00668001	0.0001670000	40	17.24	<0.0001
		Ind*Side	0.02595356	0.0000096842	2680	N/A	N/A

(B)

Subsample	Test	Component	Effect	Pillai tr.	P (param.)
Adult males	Shape MANOVA	SymmC	Status	0.83	0.0009
		AsymmC	Status	0.57	0.2202
			Side	0.94	<0.0001
Adult females	Shape MANOVA	SymmC	Status	0.51	0.0001
		AsymmC	Status	0.26	0.3604
			Side	0.9	<0.0001
Subadult males	Shape MANOVA	SymmC	Status	0.65	0.7596
		AsymmC	Status	0.6	0.3815

(B)

Subsample	Test	Component	Effect	Pillai tr.	*P* (param.)
Subadult females	Shape MANOVA	SymmC	Side	0.97	<0.0001
			Status	0.83	0.0977
		AsymmC	Status	0.49	0.8902
			Side	0.97	<0.0001